CHARACTERIZATION OF OUTBURST CHANNEL SANDSTONES IN THE PHALEN COLLIERY, CAPE BRETON, NOVA SCOTIA

Jennifer M. van der Gaag

Distribution License

DalSpace requires agreement to this non-exclusive distribution license before your item can appear on DalSpace.

NON-EXCLUSIVE DISTRIBUTION LICENSE

You (the author(s) or copyright owner) grant to Dalhousie University the non-exclusive right to reproduce and distribute your submission worldwide in any medium.

You agree that Dalhousie University may, without changing the content, reformat the submission for the purpose of preservation.

You also agree that Dalhousie University may keep more than one copy of this submission for purposes of security, back-up and preservation.

You agree that the submission is your original work, and that you have the right to grant the rights contained in this license. You also agree that your submission does not, to the best of your knowledge, infringe upon anyone's copyright.

If the submission contains material for which you do not hold copyright, you agree that you have obtained the unrestricted permission of the copyright owner to grant Dalhousie University the rights required by this license, and that such third-party owned material is clearly identified and acknowledged within the text or content of the submission.

If the submission is based upon work that has been sponsored or supported by an agency or organization other than Dalhousie University, you assert that you have fulfilled any right of review or other obligations required by such contract or agreement.

Dalhousie University will clearly identify your name(s) as the author(s) or owner(s) of the submission, and will not make any alteration to the content of the files that you have submitted.

If you have questions regarding this license please contact the repository manager at dalspace@dal.ca.

Grant the distribution license by signing and dating below.

_____   _____

Name of signatory   Date

Dalhousie University

Department of Earth Sciences
Halifax. Nova Scotia
Canada B3H 3J5
(902) 494-2358
FAX (902) 494-6889

DATE ___April 17, 1997___

AUTHOR ___Jennifer Marlene van der Gaag___

TITLE ___CHARACTERIZATION OF OUTBURST CHANNEL SANDSTONES IN THE PHALEN___

___COLLIERY, CAPE BRETON, NOVA SCOTIA___

Degree ___BSc___   Convocation ___Spring, 1997___ Year ___1997___

Permission is herewith granted to Dalhousie University to circulate and to have copied for non-commercial purposes, at its discretion, the above title upon the request of individuals or institutions.

ABSTRACT

The Phalen Colliery of New Waterford, Cape Breton, Nova Scotia is currently mining coal from the Phalen Seam of the Sydney Mines Formation, part of the offshore Carboniferous Sydney Basin. Since opening in 1984, the colliery has experienced one rock outburst (September 28, 1994) within the channel sandstone that overlies the Phalen coal seam. An outburst is a violent and extremely dangerous explosion of rock and gas, the occurrence and intensity of which depend on the presence of high lithostatic pressures, high gas pressure, high modulus of rigidity (brittleness), and very low permeability. Samples of the channel sandstone have been obtained from two cores drilled into the roof of drivage tunnels distal (PH-102) and proximal (PH-250) to the site of a recent outburst, and from the outburst sites.

Sandstones from PH-102 are fine-grained, and have evenly distributed intergranular porosity (range 6.9 to 12.1%, mean 8.5%) and variable horizontal permeability (range 0.03 to 3.02 millidarcies, mean 0.88). Sandstones from core PH-250 are very fine-grained to very coarse-grained, and show generally large amounts of compacted lithic fragments. Isolated porosity occurs within corroded potassium feldspars and pore-filling kaolinite and ranges from 4.5 to 7.7% (mean 6.5%). Horizontal permeability is low throughout the core, ranging from less than 0.01 to 0.19 millidarcies (mean 0.05).

The sandstone in PH-102 is inferred to represent a lower outburst risk. The evenly distributed intergranular porosity and higher permeability allow for a more controlled release of gas, decreasing the potential energy of the system. Under similar depth conditions, sandstone from PH-250 is inferred to have a much higher risk for outbursts. The restricted porosity within rock from PH-250 allows for the storage of methane (energy), but the very low permeability greatly restricts the escape of gas when pressure on the rocks is reduced during mining, spawning an outburst. Samples of outburst sandstones from the Phalen Colliery, #26 Colliery, and Merlebach Colliery, France, show the same characteristics of corroded potassium feldspar, kaolinite pore filling, low permeability, and predominantly intragranular porosity as rock from the base of PH-250.

Key words: Phalen colliery, channel sandstone, outburst, corroded feldspar, kaolinite pore filling, porosity, permeability

TABLE OF CONTENTS

TABLE OF FIGURES

TABLE OF TABLES

ACKNOWLEDGMENTS

Chapter 1 Introduction

1.1.0 Background

1.1.1 Phalen Colliery

The Phalen Colliery, located near New Waterford, Cape Breton is currently extracting coal from the Phalen Seam of the Sydney Mines Formation. Opened in 1984 and operated by the Cape Breton Development Corporation (CBDC), the colliery has been extracting the Phalen coal by longwall mining. Several problems have been encountered during the mining process, including water inflows, weightings, and a major rock outburst. These events can be attributed in part to a thick channel sandstone that overlies much of the seam. The channel sandstone lies from 0 m to 15 m above the Phalen Seam and can reach a thickness of 30 m. In some areas it rests directly on the coal seam (CBDC, 1994a). The sudden release of gas pressure from these sandstones during coal extraction has resulted in a violent rock/gas outburst.

1.1.2 Rock Outbursts

Rock and gas outbursts are poorly understood but extremely dangerous phenomena that occur in mines throughout the world. On September 28, 1994 a particularly violent outburst occurred in the workings of the Phalen Colliery, which resulted in serious injury to one miner. Other local mines, including #26 Colliery and Lingan, had previously experienced problems with outbursts. Several hypotheses have been proposed as to the exact mechanism of outburst initiation, but due to the large number of variables, no single comprehensive theory has been developed. Rock/gas outbursts are thought to require at least four conditions to occur: 1) high modulus of rigidity (brittleness), 2) high rock stress 3) high gas pressure in the rock, and 4) restricted permeability (P. Cain, written communication, 1996). These criteria are based on

several studies of outburst rocks and mechanisms, for example, Aston et al. (1990), Belin (1981), and Cyrul (1993). Regardless of the particular hypothesis, the physical properties of the rocks involved (i.e., porosity, permeability, petrology) are expected to play a significant role in both rock strength and the potential of the sandstones to store and release gas. To date the treatment of the petrography and porosity/permeability characteristics of the Phalen sandstones has been limited mainly to petrographic reports by AGAT Laboratories. Aston et al. (1990) have indicated some porosity values that characterize outburst sandstones from #26 Colliery. This is covered more fully in Chapter 4.

Rock/gas outbursts have been significant in several mines around the world, and are commonly associated with sandstone strata. Some of the more notable events are summarized by Jackson (1984). Ibbenbueren colliery in Germany experienced more than 100 rock/gas outbursts between 1962 and 1977. Coal mines in the former USSR (Donetz Basin) have experienced severe problems with sandstone outbursts, as have several Polish mines. Instances of floor or gob areas buckling due to outbursts of gas have also been reported. Merlebach Colliery, in Lorraine, France has experienced an outburst effect known as "shotfiring-plus", which occurs after shotfiring. Shotfiring is essentially blasting to remove coal or other strata within the mine workings. An explosive charge is placed in a "shothole" that is drilled into the coal or surrounding strata, and then detonated (Hart, 1936). "Shotfiring-plus" outbursts affect the rocks in ways very similar to, but much more severely than, normal shotfiring. Large areas of floor, roof, and drivage tunnel may be involved, and 20 to 50 times the normal volume of rock is ejected, along with the escape of thousands of cubic meters of methane (Jackson, 1984). It is typical for outbursts to increase in strength with depth, presumably due to the increased rock

stress and gas pressure.

Due to the large number of variables, there has been some difficulty in predicting whether

or not a rock is prone to outburst.   The only means currently used as an indicator of outburst risk

is disking of the sandstones in drill core. When a core disks, it is broken into several small,

stacked cylinders (i.e. disks) of rock (Figure 1.1).   Prior to the major outburst of 1994, disking

was observed in some of the cores of the channel sandstone at Phalen (6E panel, bottom) (R.

Naylor, written communication, 1997). At present, the entire channel sandstone body at the

Phalen Colliery is classified by CBDC as outburst prone (P. Cain, written communication, 1996).

It is hoped that this study will provide a means to more precisely delimit areas that might have an

especially high risk of outbursts within the Phalen mine, and possibly in other outburst-prone coal

mines.

Determining some of the factors that influence outburst risk is important from perspectives

of safety and productivity. Dangers to personnel from outbursts include being buried by

sandstone/coal ejecta, suffocation due to high methane and/or CO_2 levels, explosions of flammable

gases due to sparks, secondary outbursts or roof-falls during clean-up, and injury due to violent

movement of machinery (Jackson, 1984). During the outburst event at Phalen in 1994, a cutting

machine weighing approximately 52 tonnes was moved 2 m by the explosion (P. Cain, written

communication, 1996). A mine that is prone to outbursts can experience frequent shut-downs

due to clean-ups and risk assessment after an event. This results in major losses of productivity

for the mine, and some mine closures have occurred due to recurring outburst problems (Jackson,

1984). Lower morale and confidence of miners who are at a heightened risk for injury while on

the job will also adversely affect productivity.
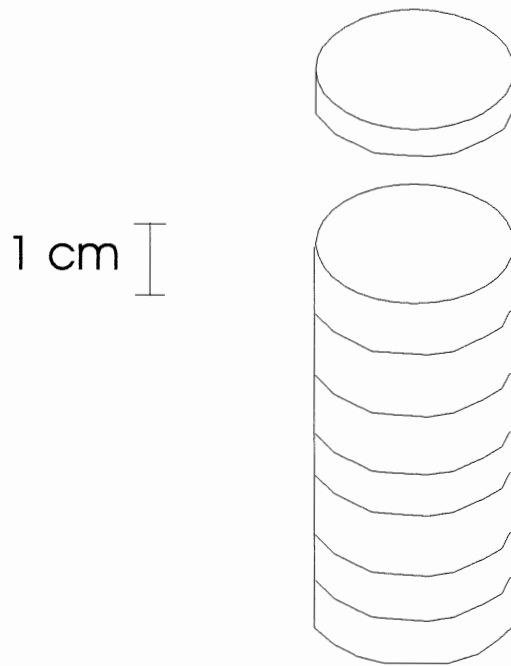
Figure 1.1 Diagrammatic representation of core disking.
Cylindrical core is broken into a "stack" of approximately
1 cm disks during drilling.

1.1.3 Geology of the Study Area: Sydney Basin and Sydney Coalfield

The Sydney Basin is a large Carboniferous basin that extends from Cape Breton to the southern coast of Newfoundland, and comprises a small onshore portion of 520 km^2 and an offshore portion of 36,000 km^2 (Hacquebard, 1983) (Figure 1.2). Rust et al. (1987) have classified the depositional environment of the basin as mainly alluvial with a progression over time from mid-braidplain to distal braid plain and finally to meandering fluvial plain. Foraminiferal evidence indicates the possibility of marine incursions into the basin (Wightman et al., 1994).

The Sydney Basin is bounded in the northwest by the Mountain Fault, and to the southeast by the Mira River-Bateston Fault. King and MacLean (1976) have described the Sydney Basin as "saucer-shaped" due to the gentle regional dip of strata toward the centre of the basin. The most prominent structural feature is the Boisdale Anticline, which divides the basin into the Ingonish and Glace Bay subbasins. Although the basin is fault bounded, most structures that affect the coal-bearing strata are interpreted to be the result of differential compaction over fault-bounded basement blocks (Gibling et al., 1987).

The Sydney Coalfield is the onshore and near offshore part of the Sydney Basin and occurs along its southwestern margin.   Stratigraphically, the section comprises two megasequences with an intervening hiatus. The lower megasequence includes the Horton, Windsor, and Canso Groups, and the upper megasequence includes the Morien Group (composed of the laterally equivalent South Bar and Waddens Cove Formations, and the Sydney Mines Formation) and overlying "unnamed redbeds" (Gibling et al., 1987) (Figure 1.3). The Sydney Mines Formation is of Late Carboniferous age, ranging from Westphalian C and D to Stephanian (Hacquebard, 1983).
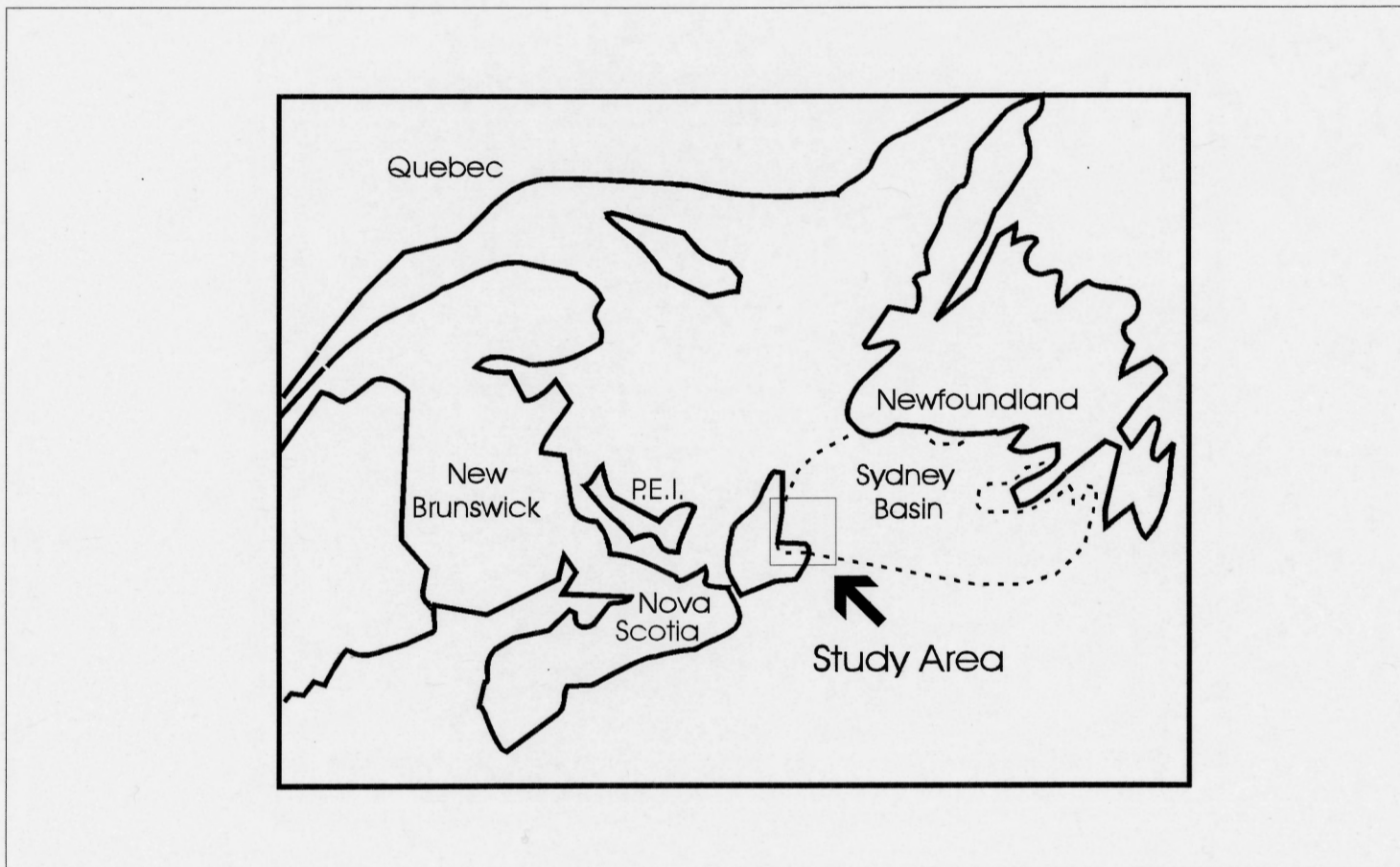
Figure 1.2 Map shows the location of the Sydney Basin and the study area (After Gibling and Bird, 1994).
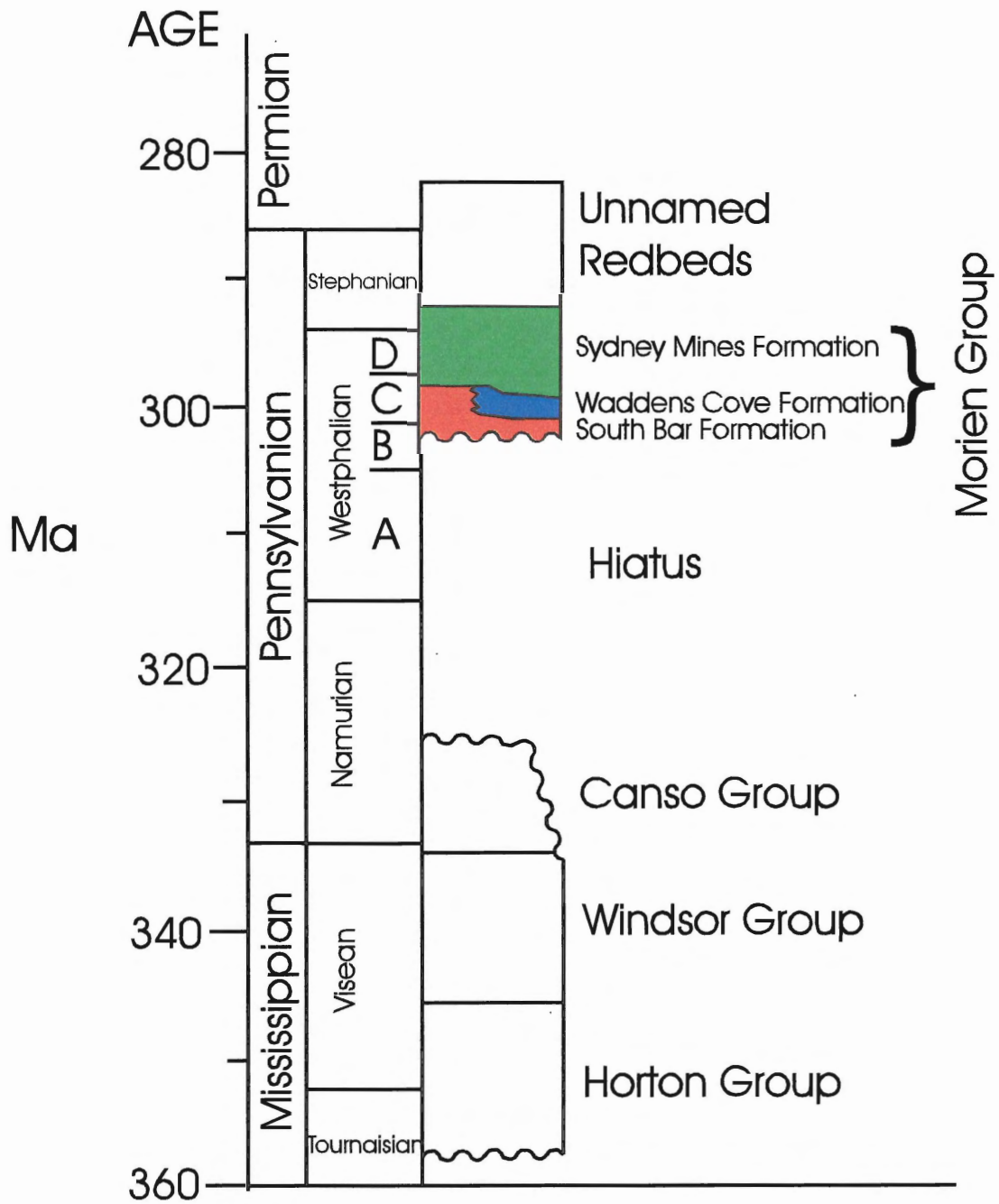
Figure 1.3 Stratigraphic column of the onshore section of the Sydney Basin. The Hiatus was approximately 22 ma. (After Gibling et al., 1987)

It crops out in several coastal sections, and extends northward out underneath the Atlantic Ocean (Figure 1.4).

The Sydney Mines Formation is predominantly mudstone (50%), sandstone and minor carbonate (Gibling et al., 1987), but contains several economic coal seams including the Phalen Seam which underlies the zone of interest to this project (Figure 1.5). The Phalen Seam was probably deposited in a fluvially-dominated environment where peat accumulated in extensive swamps on a "low gradient alluvial plain" (Rust et al., 1987). All the coal in the Sydney coalfield is classified as high volatile "A" bituminous, although the rank increases both eastward and with depth (Hacquebard, 1983).

1.1.4 Previous Work

King and MacLean (1976) determined the extent of the Sydney Basin based on geophysical methods, and Hacquebard (1983) has carried out extensive work on the coal. Gibling and others have contributed extensively to work on the stratigraphy of the Sydney Basin, for example Gibling et. al (1987), Rust et al. (1987) and Gibling and Bird (1994). The majority of work on outbursts in the Sydney coalfield has been carried out by Aston et al. (1990) and Kullman and Barron (1990a,b). P. Cain (written communication, 1996) has summarized Canadian research to date on outbursts, with particular concentration on the Sydney Coalfield. CBDC has produced several internal reports on conditions at the Phalen mine, for example, Cape Breton Development Corporation (1994a,b). AGAT Laboratories has described the petrology and porosity/permeability characteristics of several samples of the channel sandstones from the Sydney Coalfield, for example AGAT (1995).
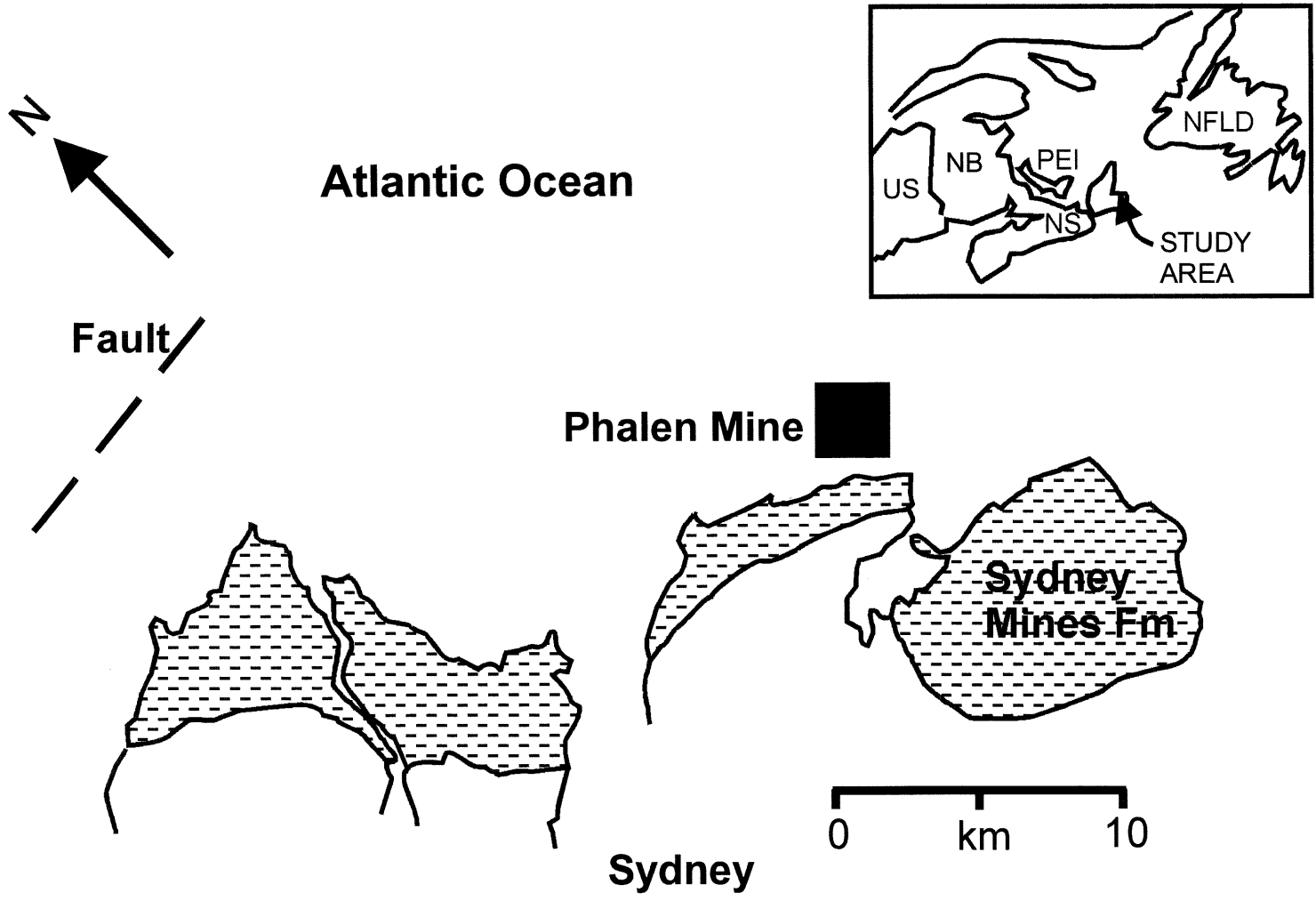
Figure 1.4 Map showing occurrence of Sydney Mines formation and study area. Inset shows regional area (After Gibling and Bird, 1994)
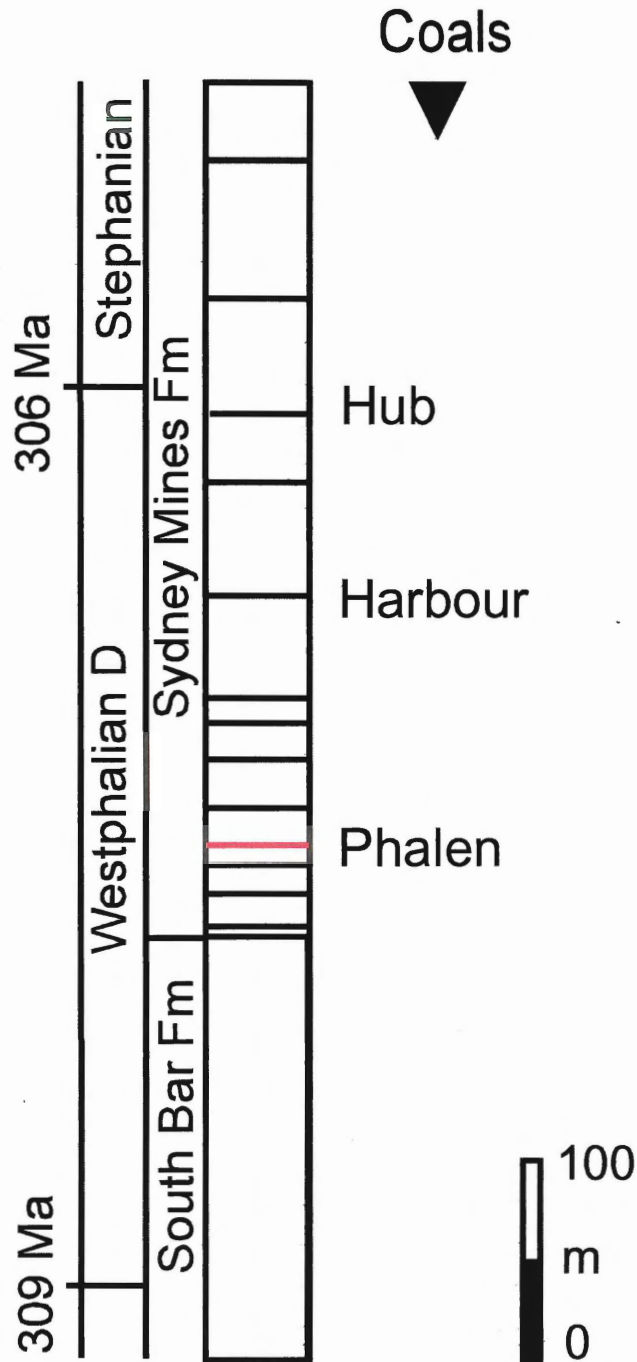
Figure 1.5 Stratigraphic section of the Sydney Mines Formation showing coals. Phalen seam is highlighted in red.

1.2.0 Objectives

This thesis characterizes the petrology, porosity, and permeability of outburst channel sandstones at the Phalen Mine. Due to the large number of factors that influence outbursts, it is difficult to say with certainty to what extent petrology influences outburst risk. Finding significant petrologic and or porosity/permeability differences could lead to the development of a finer classification of outburst risk within the channel sandstone.

This study is part of a larger investigation of the problems associated with geology at the Phalen Mine. A larger study on the hydrogeology and geochemical evolution of the Phalen formation water is currently being conducted in an effort to determine the source of the large water inflows into the mine. Work is also ongoing by Kullmann and Barron to develop outburst models for the Sydney Coalfield.

1.3.0 Scope

This project is limited to the Phalen Colliery itself, and it is unknown to what extent the results can be reliably extrapolated to other mines, or even to other parts of the Sydney Coalfield. Comparisons with an outburst sandstone from Merlebach Colliery (France), and from #26 Colliery, which have experienced similar outbursts, will provide a basis for discussion of this point. The scope does not include determining the cause of outbursts or developing any hypothesis about outburst mechanisms. There are many factors that affect this, most of which are in the realm of engineering. Characterization of the samples is limited to common petrographic microscope techniques, microprobe analysis, environmental scanning electron microscopy, point counting, and porosity and permeability data. Samples are limited to two cores from the roof of drivage tunnels in the Phalen mine, and outburst samples from Cape Breton and France.

Chapter 2 Methodology

2.0.0 Introduction

The data set for this thesis is derived primarily from two cores drilled into the roof of drivage tunnels in the Phalen mine, and from hand samples from #26 Colliery and Merlebach Colliery. Several methods were used to analyze the samples in order to determine as complete a characterization as possible. The emphasis of the testing was to determine petrology as well as porosity and permeability characteristics of the outburst sandstones, and how these characteristics might affect outburst risk.

2.1.0 Petrology

2.1.1 Stratigraphy

Stratigraphic logs of the Phalen cores were produced by R. Naylor of the Nova Scotia Department of Natural Resources (DNR). Logging was done on a centimetre scale, with particular attention to the large channel sandstone. A dilute acid solution was used to test for the presence of carbonates. Grain size was determined visually.

2.1.2 Petrography

The selection of samples from the two Phalen cores, PH-250 and PH-102 was based partly on rock density curves obtained from Multi-Sensor Core Logger (MST) analysis and stratigraphic logs, and partly on the location of plugs that had previously been removed from the core boxes and analyzed by the Cape Breton Development Corporation (CBDC). The sandstones were classified according to the Udden-Wentworth grain size scale and Folk (1968) sandstone classification. Eighteen 0.03 mm thin sections were cut from the core plugs and stained with blue epoxy to emphasize porosity. The sections were examined for mineralogy and texture, including

structures, stratification, porosity/permeability, cementation and alteration (diagenetic

characteristics). Point counting was used to determine the relative proportions of mineral species

present in the thin sections. Five hundred points were counted on each section using a Swift,

model F automatic point counter. Porosity values obtained from point counting are not

representative of actual rock porosities. Most pore spaces were at least partially filled with clay

minerals (e.g. kaolinite patches) in which case the mineral was counted, and not the porosity.

Three thin sections cut and described by AGAT Laboratories were examined, but not included in

the point count. These sections were cut parallel to bedding, whereas the other 18 sections were

cut perpendicular to bedding.

2.1.3 Environmental Scanning Electron Microscope and Microprobe

The Environmental Scanning Electron Microscope (ESEM) at Bedford Institute of

Oceanography (B.I.O.) was used under the supervision of K. Moran and F. Thomas to determine

clay and pore morphology of the sandstones and to generate high magnification images of these

features. Appendix A details some specifications of the ESEM and analytical procedures. Some

compositional analysis of clay materials was carried out using energy dispersive spectrometry

(EDS) detector on the ESEM. Compositional analysis of corroded feldspar grains was performed

under the supervision of R. MacKay using the JEOL 733 Superprobe in the Dalhousie

Microprobe Laboratory.

2.2.0 Porosity and Permeability

2.2.1 Porosity

Porosity can be measured indirectly using the MST. This instrument measures the

attenuation of gamma rays directed through the core and uses this data, along with core diameter,

to calculate rock density values. Traditionally, the MST has been used only for determining the density of soft sediment cores, so porosity values obtained from this analysis should be compared, for accuracy, with porosities determined by more conventional methods (e.g. data from AGAT Laboratories of Calgary). Porosity logs can be obtained from the MST density curves using bulk and grain density measurements. Bulk density values were calculated using the saturated and dry weights of 2 cm core plugs and their measured volumes. Due to difficulties with calibration, only the density logs are available at this time. Porosity values discussed in later chapters are those data obtained by AGAT Laboratories (AGAT, 1995).

Porosity is important to the classification of the Phalen sandstones as previous studies have indicated that both void space and permeability play a significant role in outburst potential (Kullman and Barron, 1990a). Appendix B deals more fully with the specific function and procedures used with the MST.

2.2.2 Permeability

The degree of interconnectedness of the pore spaces in the Phalen channel sandstone is important in that it determines how readily gas can escape from the rock after a sudden release of pressure. This author makes only qualitative estimates of permeability, based on traces of blue epoxy present in the thin sections. Permeability data for samples from PH-102 and PH-250 were measured by AGAT Laboratories (AGAT, 1995).

Chapter 3 Results

3.0.0 Introduction

Data describing outburst sandstones at the Phalen Colliery were obtained primarily from two cores drilled into the roof of drivage tunnels; one distal (PH-102) and one proximal (PH-250) to the location of a violent outburst that occurred on September 28, 1994 (Figure 3.1). The majority of information was collected from thin sections and core plugs for which porosity/permeability data were calculated. This chapter summarizes the petrography, and porosity and permeability data collected from the Phalen cores, as well as samples from #26 Colliery and Merlebach Colliery.

3.1.0 Stratigraphy

Core PH-250 is 23.53 m long and classified almost entirely as massive channel sandstone with a 0.5 m very fine-grained sandstone interval (possibly a "bayfill" sediment body) at the base, and some intermittent siltstone layers (Figure 3.2). The channel sandstone fines upward from medium-coarse to fine-grained and shows occasional siderite bands and clasts, and some siltstone clasts. Some carbonate cement occurs in the lower third of the core. Structures within the core include ripple cross-laminae with and without siderite, and planar carbonaceous laminae with siderite. The ripple cross-laminae occur most commonly in the top 6 m of core, whereas the planar laminae are found near the middle of the core. Within the channel sandstone individual beds range in thickness from approximately 0.1 m to 1.3 m. From approximately 9 m to 10.3 m there is a series of alternating 0.2 m thick massive beds and beds with ripple cross-laminae (with and without siderite). These beds could increase the bulk permeability of this otherwise almost entirely massive sandstone. Disking, which is typically recognized as a sign of outburst risk,

Phalen Mine Plan

Outburst

Ph-250

Ph-102

10E

9E

2C

8E

1C

7E

6E

5E

3W

4E

2W

3E

1W

2E

1E
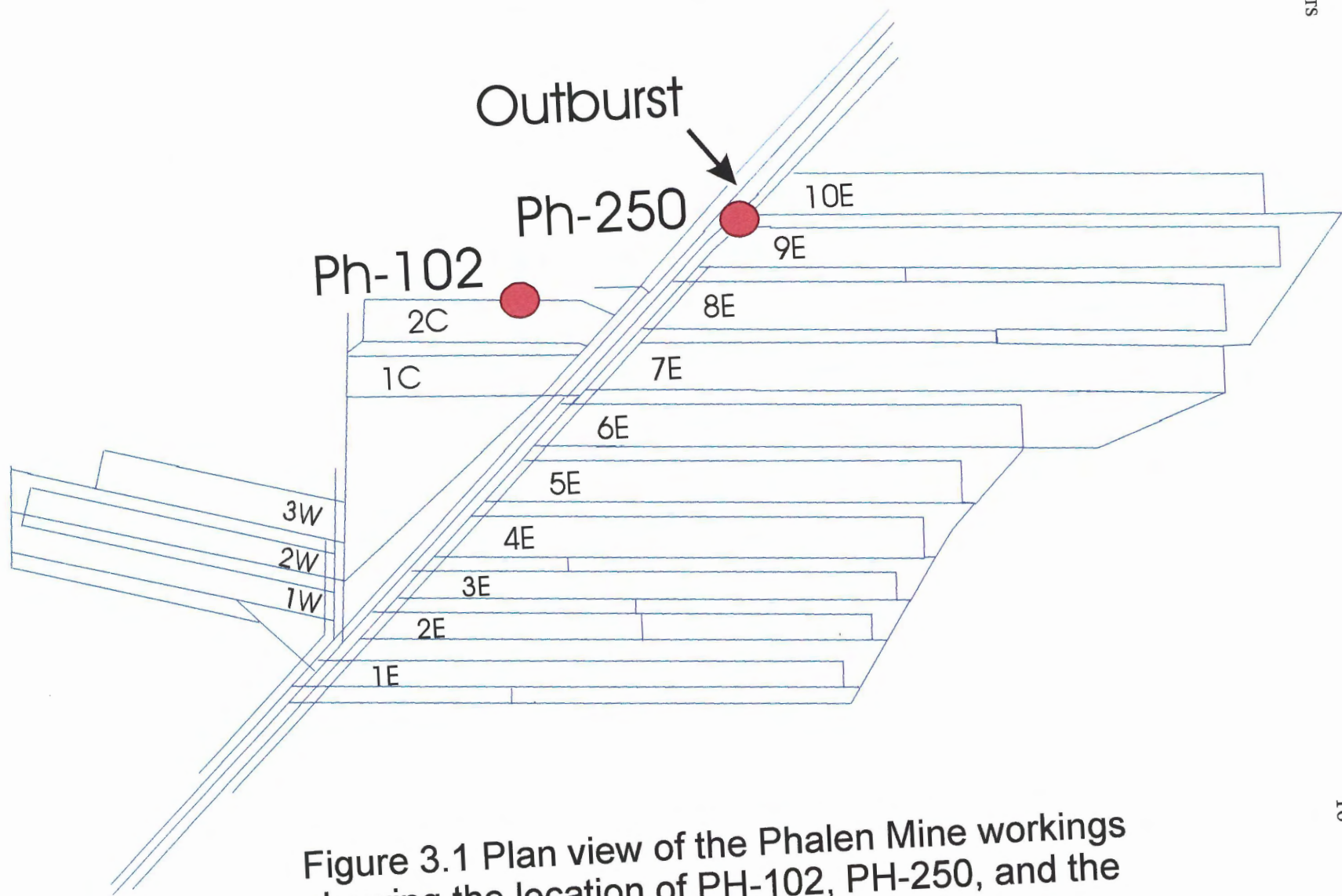
Figure 3.1 Plan view of the Phalen Mine workings showing the location of PH-102, PH-250, and the 1994 outburst.

Phalen 250
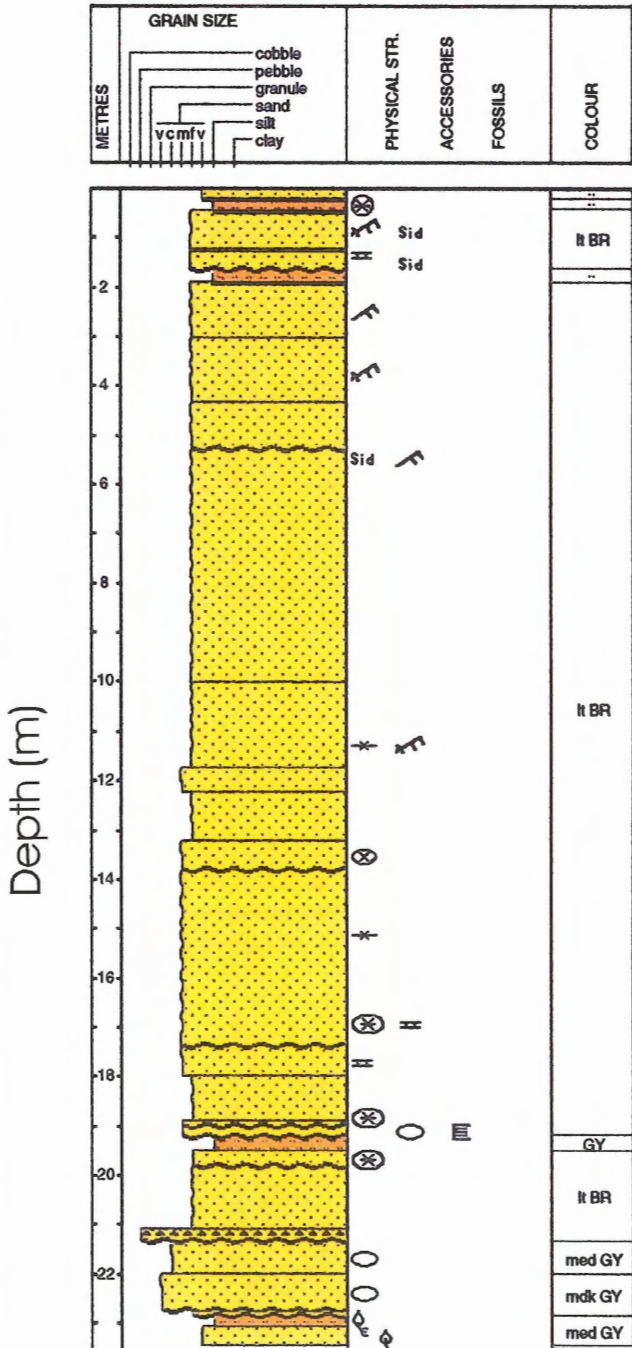
Depth (m)

Figure 3.2 Stratigraphic log of core PH-250. This core is almost entirely massive channel sandstone. Sample depths are indicated below.

Sample Depths (m)					
250-15	6.6	FGLP	250-5	21.5	CGLP
250-12	11.3	FGLP	250-3	22.0	CGLP
250-10	14.0	LAG	250-1	22.5	CGLP
250-6	20.5	FGLP			

LEGEND

sandstone	claystone	coal	limestone	silty shale	
siltstone	organic shale	breccia			

⎯⎯ Sharp   〰 Undulating

⊨ - Calcareous	Sid - Siderite	Py - Pyrite
⚲ - Ripple laminae	✳ - Planar carbonaceous	⊗ - Siderite clast
⊛ - Calcareous clast	◯ - Lithic clasts	⎯ - Carbonaceous
⊔ - Lenticular		目 - Disking
⊙ - Ostracods	⚘ - Plant Remains	◠ - Bivalves
⚲ - Root		
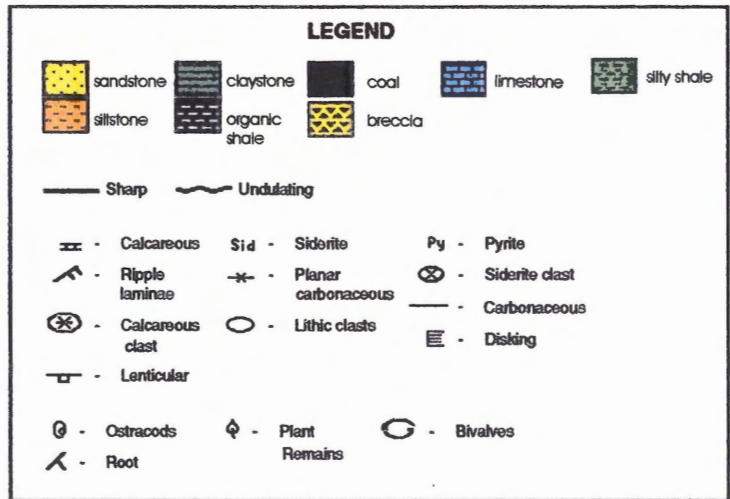
occurs in only a small section of core PH-250 (approximately 0.05 m) (P. Cain, written

communication, 1996).

Core PH-102 is 30.18 m long with channel sandstone occurring in the bottom two thirds

of the core (Figure 3.3). The basal 0.27 m is siltstone, which is overlain by approximately 9 m of

channel sandstone, then approximately 4 m of interbedded of siltstone and fine-grained sandstone

(possibly an abandoned channel fill). This section is overlain by approximately 6.5 m of channel

sandstone, which is capped by 10 m of finer-grained strata composed of limestone, calcrete, silty

mudstone, mudstone, fine-grained sandstone and the Backpit coal. PH-102 shows more internal

structure than PH-250. Planar carbonaceous laminae (with and without siderite) are found

throughout most of the channel sandstone. Lenticular laminae or streaks and ripple cross-laminae

occur from approximately 18 m to 20 m in very fine-grained sandstone; ripple cross-laminae occur

at approximately 22 m. Within the channel sandstone the thickness of individual sandstone beds

ranges from approximately 0.10 m to 1.5 m. From approximately 14 m to 17 m there are

alternating massive beds and beds with planar carbonaceous laminae (with siderite), ranging in

thickness from 0.08 m to 0.50 m. Disking does not occur in PH-102.

3.2.0 Petrography

Point counts performed on samples from the two Phalen cores provide detailed

petrography that is not available from the stratigraphic logs. The point count data are

summarized in Appendix C. Quartz content was high for all of the samples, usually exceeding

60%. Generally the most abundant constituents following quartz were lithic fragments and

detrital clay matrix (component minerals not identifiable in thin section), both of which commonly

show alteration to muscovite (illite?) or sericite. Clays also occur as pore-filling/replacement

Phalen 102
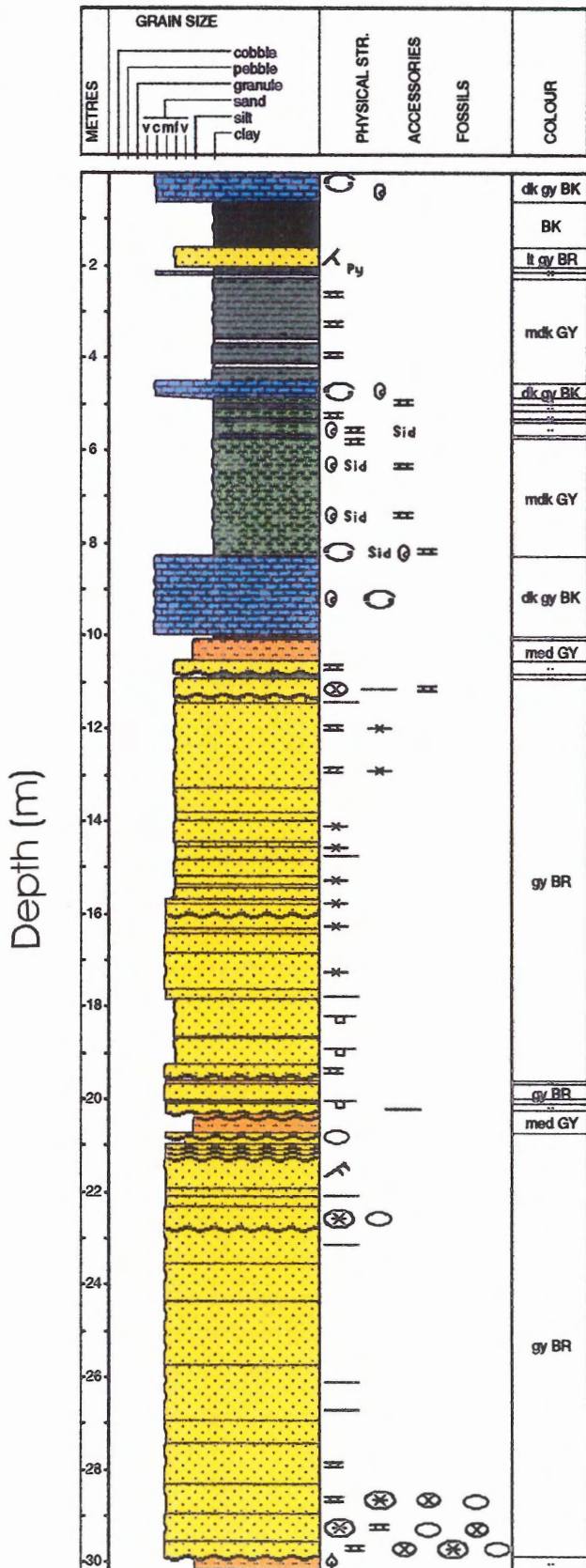
Figure 3.3 Stratigraphic log of core PH-102. From 11m to 30m is mainly channel sandstone. Sample depths are indicated below.

Sample Depths (m)					
102-13	12.0	FGLP	102-6	21.2	FGHP
102-12	14.5	FGHP	102-5	22.4	LAG
102-11	17.0	FGHP	102-3	25.7	FGHP
102-9	19.0	FGHP	102-1	29.2	LAG

LEGEND

sandstone	claystone	coal	limestone	silty shale
siltstone	organic shale	breccia	calcrete

—— Sharp   ⌇ Undulating

≡ - Calcareous	Sid - Siderite	Py - Pyrite
⌁ - Ripple laminae	⚹ - Planar carbonaceous	⊗ - Siderite clast
⊗ - Calcareous clast	◯ - Lithic clasts	—— - Carbonaceous
⊤ - Lenticular		⊞ - Disking
◷ - Ostracods	⚲ - Plant Remains	◯ - Bivalves
⌁ - Root		

minerals (e.g. kaolinite). Lithic fragments are predominantly mudstone, although a significant

portion are schist or chert fragments. Some of the "mudstone lithics" may have originated as

Carboniferous pedogenic mud aggregates that were reworked into the channel sandstones (Rust

and Nanson, 1989; M.R. Gibling, personal communication, 1997). Metamorphic quartz is

common in the basal portion of PH-250. Feldspar is rare to occasional in the sandstones, and

most commonly occurs as highly corroded potassium feldspar, sometimes in association with

calcite, kaolinite or both. Albite is very rarely present as small, pristine grains usually showing

well-developed albite twinning. Cements common in the samples were siderite, clay (kaolinite,

illite), and calcite, with evidence of quartz overgrowths in some samples.

Data obtained from point counting, a series of petrographic descriptions and AGAT

reports are used to divide the samples into five categories based on grain size, porosity, and

occurrence (outburst or non-outburst). Divisions were made on the basis of AGAT porosity

values (i.e. not the point count values) and, in one case, a visual estimate of porosity. The

petrographic categories are: lag deposits (LAG), fine-grained low-porosity sandstones (FGLP),

fine-grained high-porosity sandstones (FGHP), coarse-grained low-porosity sandstones (CGLP),

and sandstones that have outburst (OBT). Figure 3.4a shows examples of core typical of LAG,

FGLP, FGHP, and CGLP. Figure 3.4b shows examples of outburst sandstone. Figure 3.5 shows

these samples plotted on a ternary diagram, according to Folk (1968). General porosity and

permeability values were noted for each group are discussed fully in a later section.

3.2.1 Lag Deposits

Lag deposits (LAG) are very poorly to poorly sorted, very coarse-grained sandstones to

conglomerates. These rocks are characterized by subangular to angular lithic and sideritic clasts,

A

Figure 3.4 Samples of petrographic groups. (A) PH-250-1 and PH250-5 belong to group CGLP. PH250-10 belongs to group LAG. PH250-15 belongs to group FGLP. Sandstones in FGHP are superficially almost identical to sandstones in FGLP group, and are not shown.

B

Figure 3.4 (B) Samples of OBT group. Sample on left of photograph is from Merlebach colliery, France. Sample on right is from the major Phalen outburst. Field of view is 22 cm.

Q
Quartzarenite

Subarkose   Sublitharenite

Arkose

Lithic Arkose

Feldspathic Litharenite

Litharenite

F   3:1   1:1   1:3   RF

Folk (1968)

LEGEND
◇ LAG
□ FGLP
△ FGHP
○ CGLP
⬠ OBT

Quartz

95

75

Feldspar   Rock Fragments
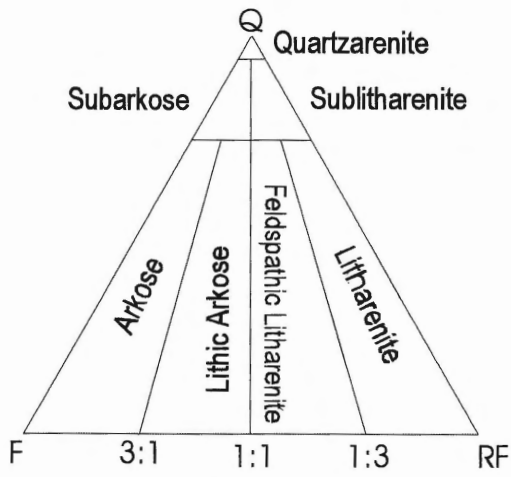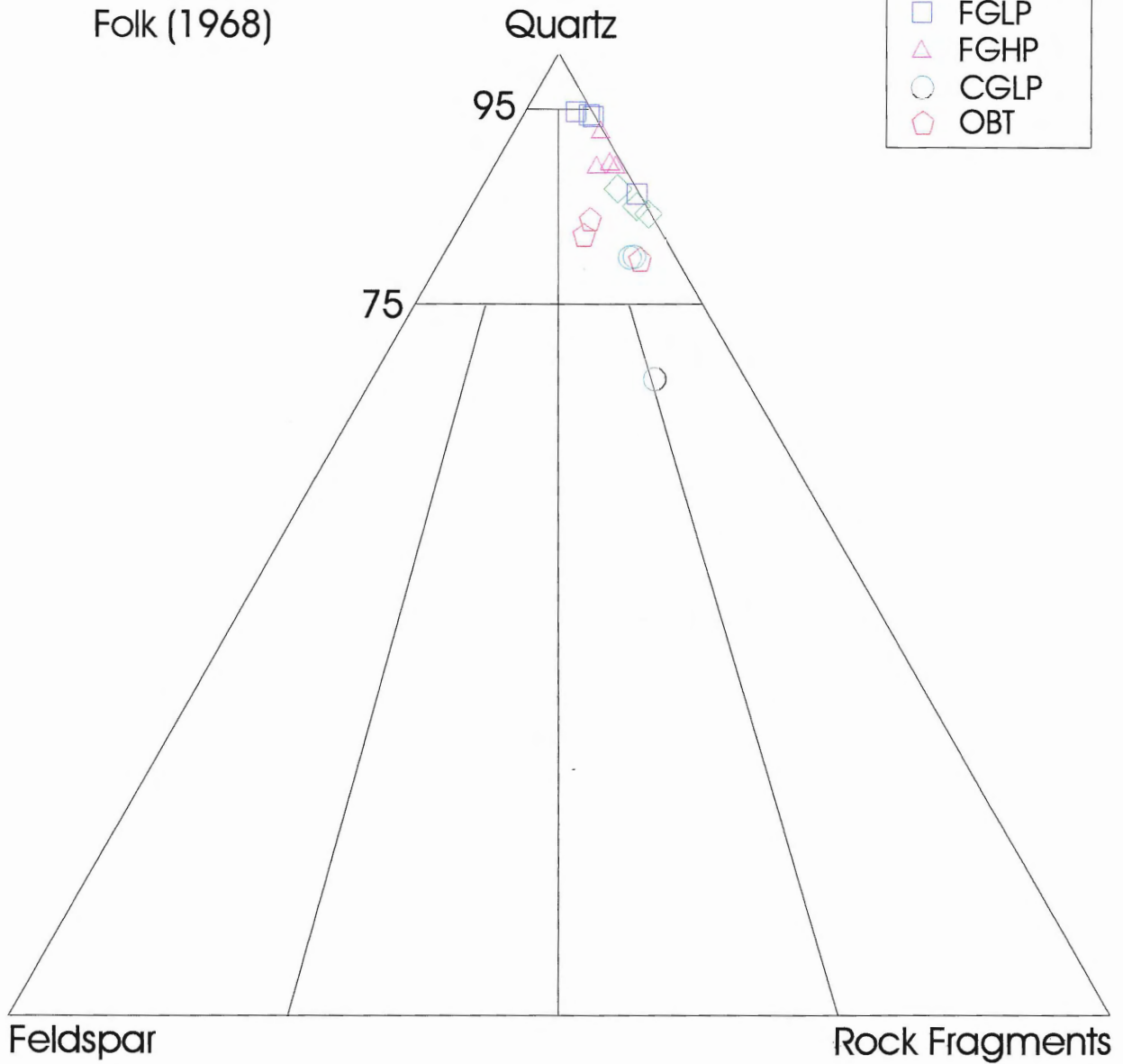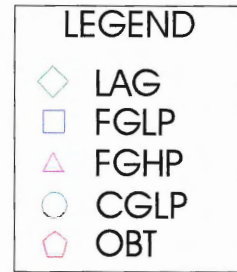
Figure 3.5 Ternary plot of Phalen (PH-250, PH-102) and outburst samples by petrographic group (Folk, 1968).

ranging in size from coarse-grained sand to small pebbles. Lithics present include chert,

clay/siltstone, schistose metamorphic rock, igneous rock and soil aggregates. The matrix is

predominantly fine-grained (average 0.1 to 0.2 mm), subangular to subrounded monocrystalline

and polycrystalline quartz (Figure 3.6). All three samples in this group have predominantly

calcite cement (poikilotopic, large crystals enclosing several framework grains), with PH250-10

having the most calcite of any sample at approximately 35%. Some quartz overgrowths are

present. Minerals present but not included in the point count include zircon, olivine, ferruginised

grains, glauconite, phosphatic bone fragments, muscovite and biotite. Glauconite occurs as a

small number of rounded, bright green grains (pellets ?), approximately 0.2 mm in size. Both

detrital and authigenic (kaolinite, illite) clays are present. Porosity is mainly intergranular, with

some secondary porosity in skeletal feldspar and clay patches. Though numerical porosity values

average 8.8%, almost no blue epoxy was absorbed. The reason for this is unknown. Permeability

is restricted. This rock type occurs both in PH-250 (sample 10) and in PH-102 (samples 1 and 5)

at the bottom of some channel sandstone storeys. This rock type occurs only in thin, localized

intervals in the core and will not be considered in detail.

3.2.2 Fine-grained Low-porosity Sandstones

The fine-grained (average .15 mm) low-porosity (FGLP) sandstones are well to

moderately sorted, mature sublitharenites (Figure 3.7). Quartz grains are subrounded to

subangular, monocrystalline and polycrystalline with some overgrowths. The quartz overgrowths

are separated from the quartz nucleus by clay pellicles. Some of the overgrown grains have

leached overgrowths that lack euhedral form, and may be recycled. Lithic fragments of schist,

igneous rock, quartzite, clay/siltstone, soil, and chert are present. Muscovite grains commonly
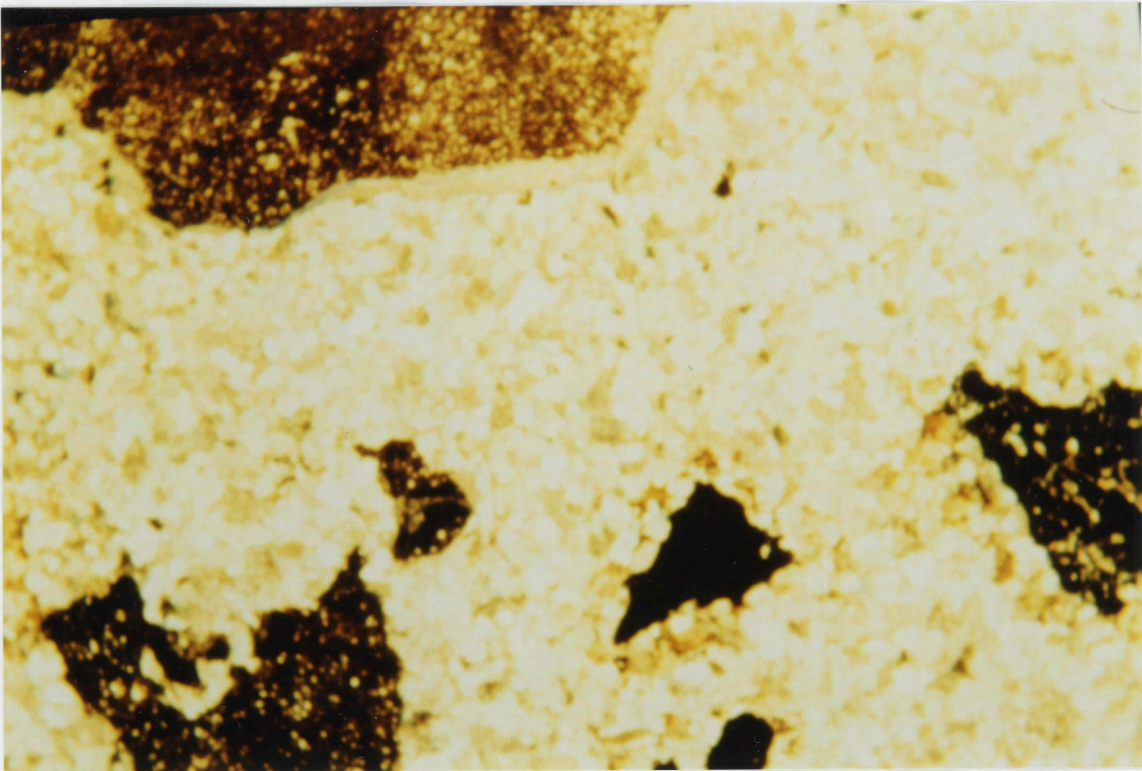
Figure 3.6 Example of LAG group. The sample shows poor sorting, with pebble-sized siderite and opaque clasts in a fine-grained quartz matrix (magnification 6.3x).
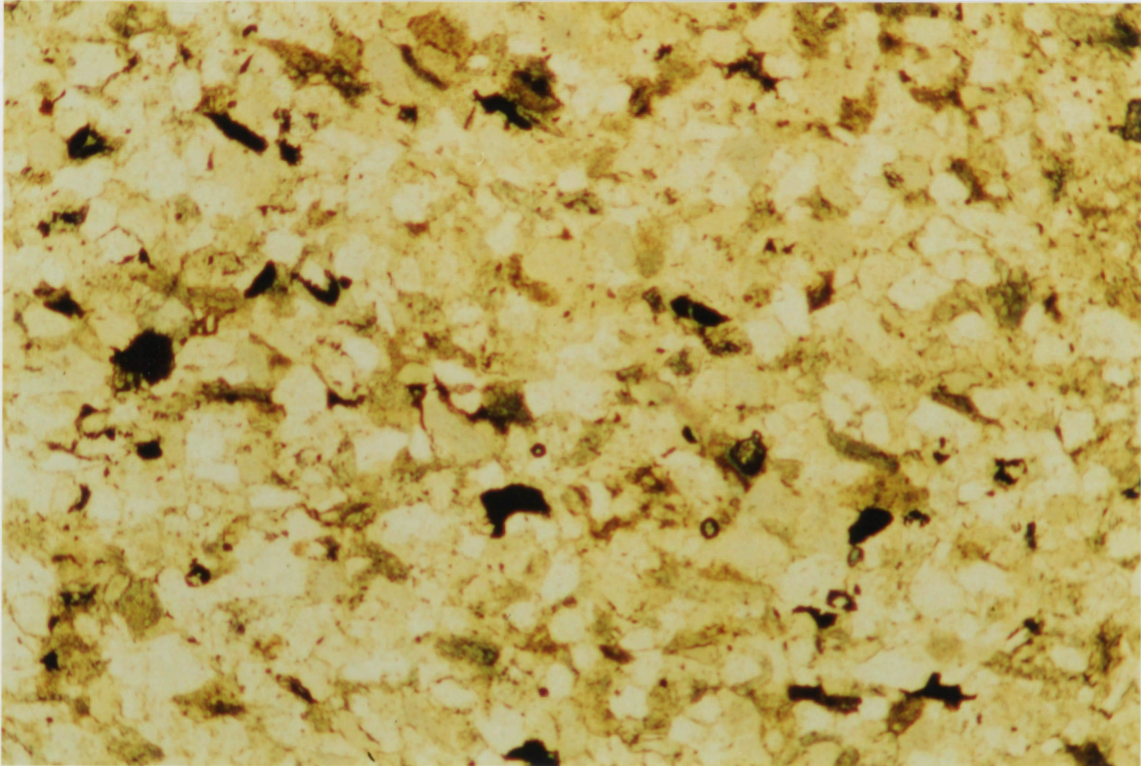
Figure 3.7 Example of FGLP group. The sample is a fine-grained, well sorted sublitharenite. Lithic grains are abundant, and porosity and permeability are low - note the absence of blue epoxy (magnification 6.3x).

show deformation due to compaction. Framework grains are slightly separated by abundant

detrital and authigenic clays (illite). Sericite occurs as an alteration product within the matrix

clays (AGAT, 1995). In this group feldspar and kaolinite represent less than 2% of the total point

count. Minerals present that were not indicated in the point count include zircon, muscovite,

chlorite, pyrite and glauconite. Although the samples were mounted in blue epoxy, they show

almost no porosity in thin section. Numerical porosity values (AGAT) are similar to the following

group, FGHP, but due to the lack of epoxy absorption, these samples are classified separately (i.e.

visual inspection vs. solely AGAT data). The main difference between the FGLP and the FGHP

group appears to be the kaolinite concentration. FGLP has, on average, 1.2% kaolinite, whereas

FGHP has 10.6%. It is possible that the epoxy is more readily absorbed into kaolinite filled pores.

There are rare, extremely degraded remnant feldspars with associated intragranular (skeletal)

porosity. Permeability is quite low. This type of sandstone occurs in the uppermost sections of

PH250 (samples 6, 12, and 15) and PH102-13.

3.2.3 Fine-grained High-porosity Sandstones

The fine-grained to very fine-grained (average 0.1 to 0.3 mm) high-porosity (FGHP)

sandstones are well sorted, mature sublitharenites distinct from the fine-grained low-porosity

sandstones in that they exhibit evenly distributed intergranular porosity (Figure 3.8). Quartz

grains are subangular to subrounded, monocrystalline and rarely polycrystalline, with abundant

overgrowths. Lithic fragments include metamorphic (schist) grains, clay/siltstone, igneous rocks,

and chert. "Fresh" plagioclase or potassium feldspar is rare, but there is evidence of severe

degradation of potassium feldspar to kaolinite. Clay matrix is abundant resulting in only moderate

contact between framework grains. Authigenic clays present include kaolinite and illite.
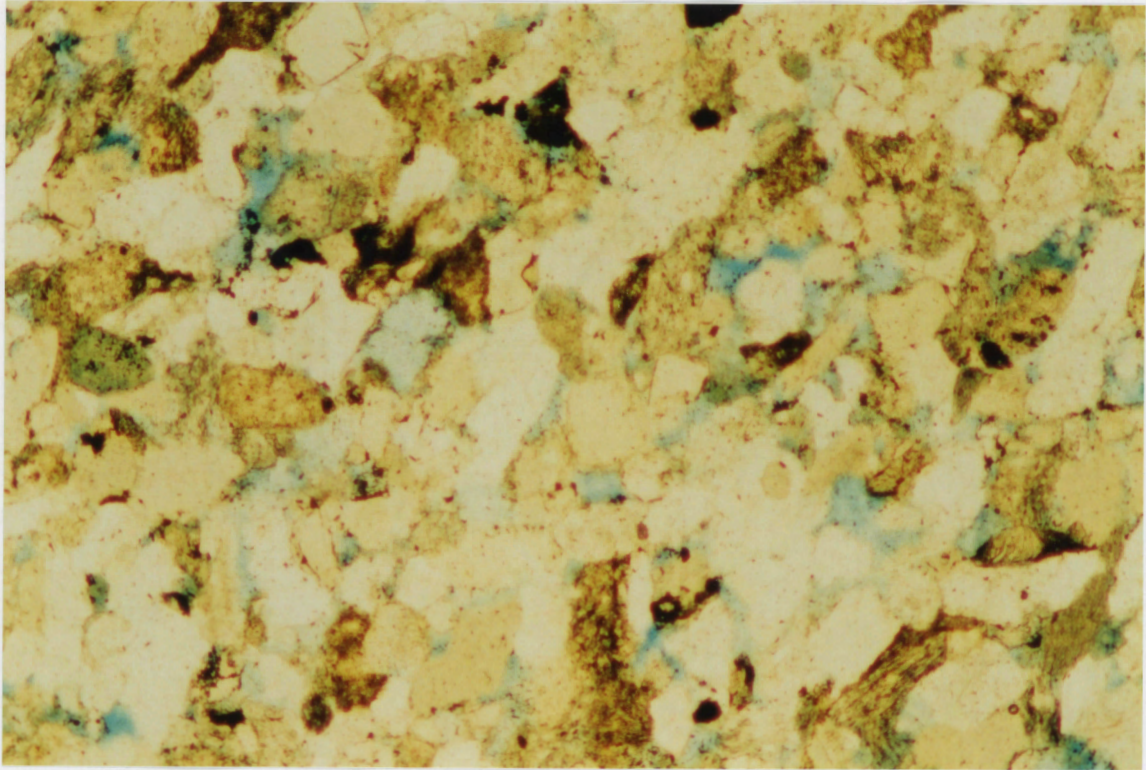
Figure 3.8 Example of FGHP group. This is a fine-grained, well sorted sublitharenite. Lithic grains are abundant, and porosity (blue areas) and permeability are good. Kaolinite is a common pore-filling mineral (magnification 32x).

Minerals present in the rock but not counted in the point count include biotite, muscovite, zircon, and ferruginised grains. Carbonate occurs in irregular, approximately grain-sized patches, often as a replacement of feldspar. Porosity is generally intergranular with associated kaolinite, which is much more common (10.6% vs. 1.2% kaolinite) than in the low porosity rocks. As mentioned in the previous section, AGAT porosity values are similar for FGHP and FGLP, although FGHP absorbed much more blue epoxy. Microporosity is associated with matrix clay patches. Permeability is generally higher than in the fine-grained low-porosity group, but still low overall. These sandstones occur only in PH-102 (samples 3,6,9,11, and 12).

3.2.4 Coarse-grained Low-porosity Sandstones

The coarse-grained to small granule-size (average 1 mm) low-porosity (CGLP) sandstones are poorly sorted, poorly cemented, sub-mature litharenites (Figure 3.9). Quartz grains are angular to subangular, monocrystalline and polycrystalline with highly sutured grains. Lithics are abundant and include metamorphic (schist) and igneous rock, quartzite, chert, clay/siltstone, and clay aggregates. Some lithics show deformation due to compaction, as do muscovite grains. Large grains of corroded potassium feldspar (including microcline) are present in this group (Figure 3.10). They show evidence of preferential dissolution along cleavage intersections and at grain edges, resulting in the formation of secondary porosity. Smaller, rare grains of unaltered albite are also present. Much of the secondary porosity in the feldspar grains was filled by calcite and kaolinite. AGAT (1995) identified dolomite and calcite in the feldspars, through staining techniques. Matrix clays are mostly unidentifiable as to group, and their distribution is patchy so framework grains are commonly in contact with each other. Siderite commonly occurs as a cement, forming rims around framework grains, and in patches. Other minerals present include
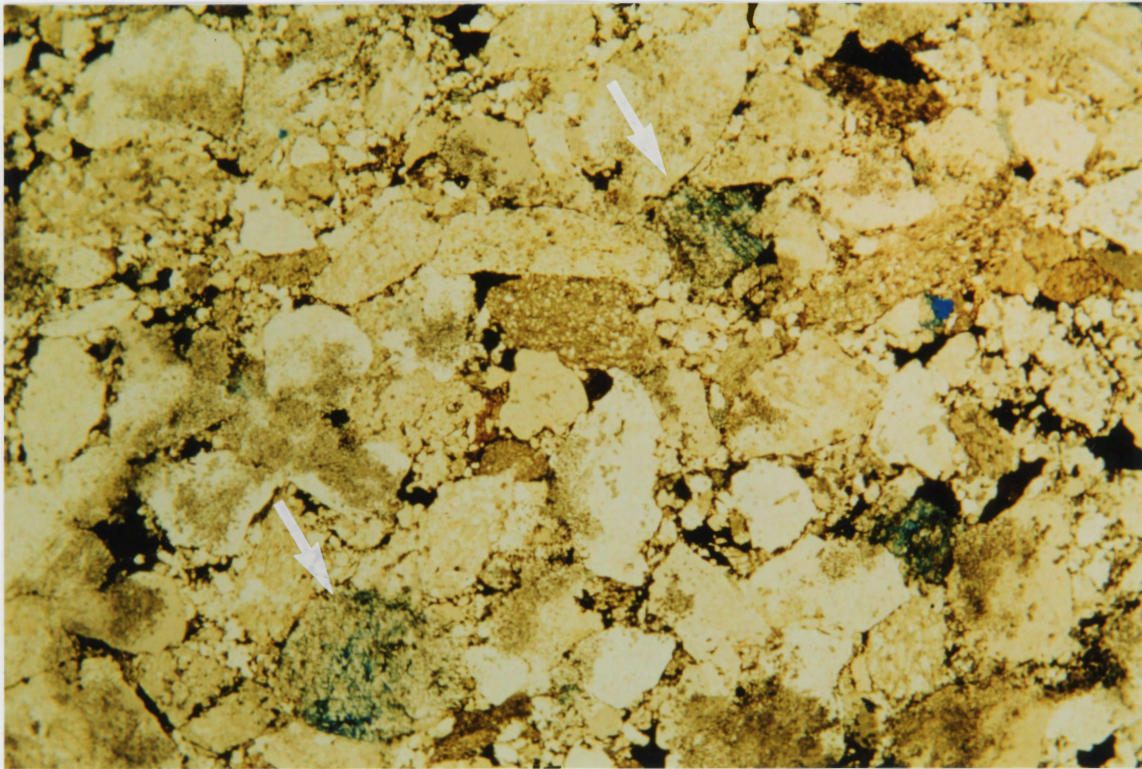
Figure 3.9 Example of CGLP group. This is a coarse-grained, poorly sorted, sub-mature litharenite. Lithic grains are abundant. Arrows indicate corroded feldspar grains with intragranular porosity. Black rims around grains are siderite (magnification 6.3x).

A
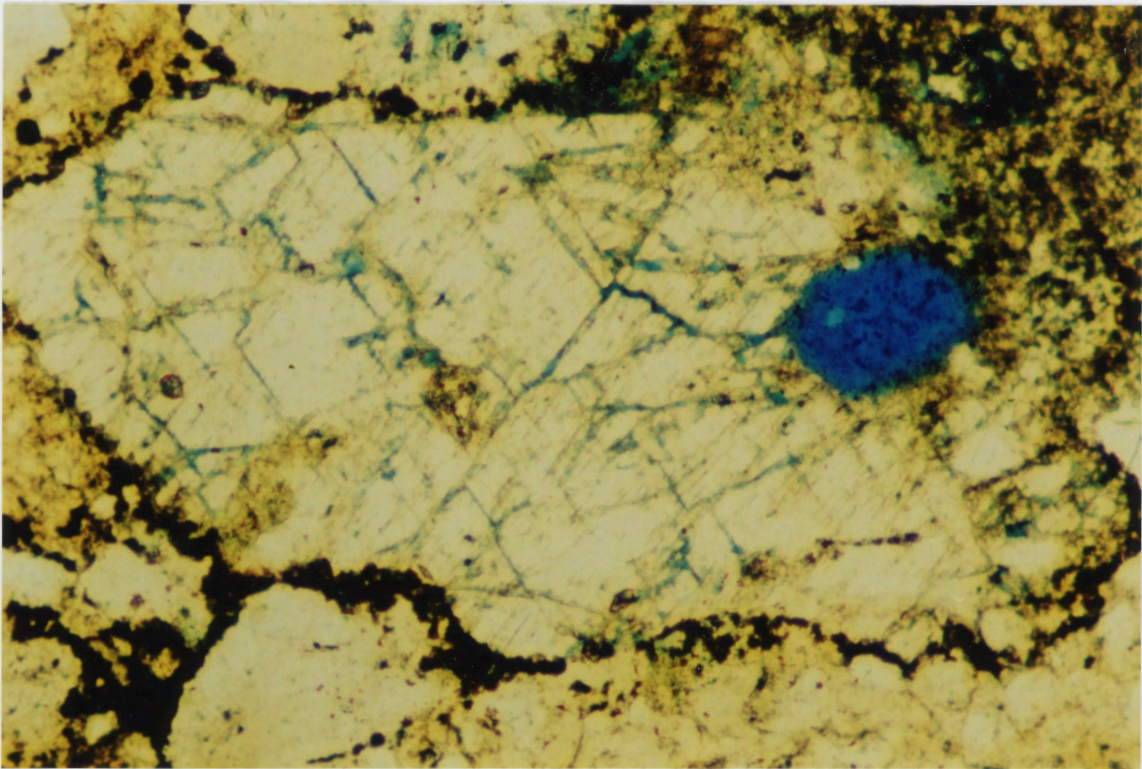
B
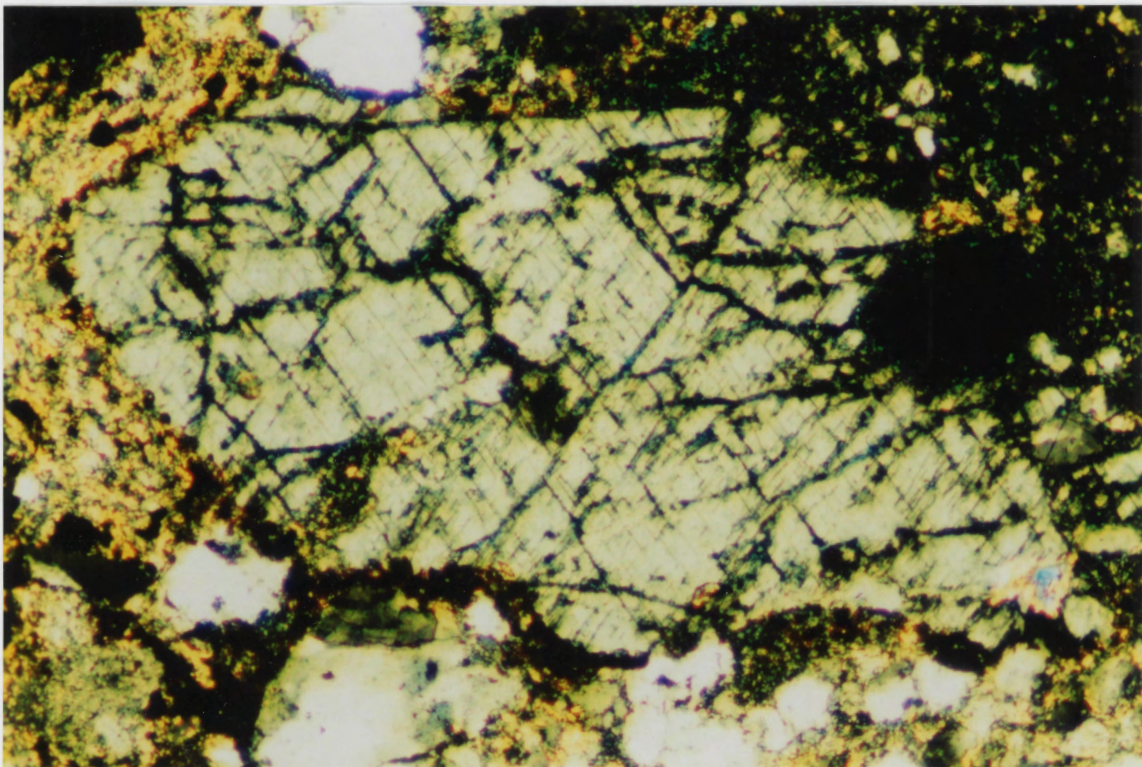
Figure 3.10 Corroded feldspar grains. (A) Feldspar grain rimmed by siderite. It shows preferential dissolution (blue) along cleavage intersections and replacement by kaolinite (magnification 64x, PPL). (B) Same as (A), but with crossed polars. Note calcite cement (high birefringence) in bottom right corner.

C
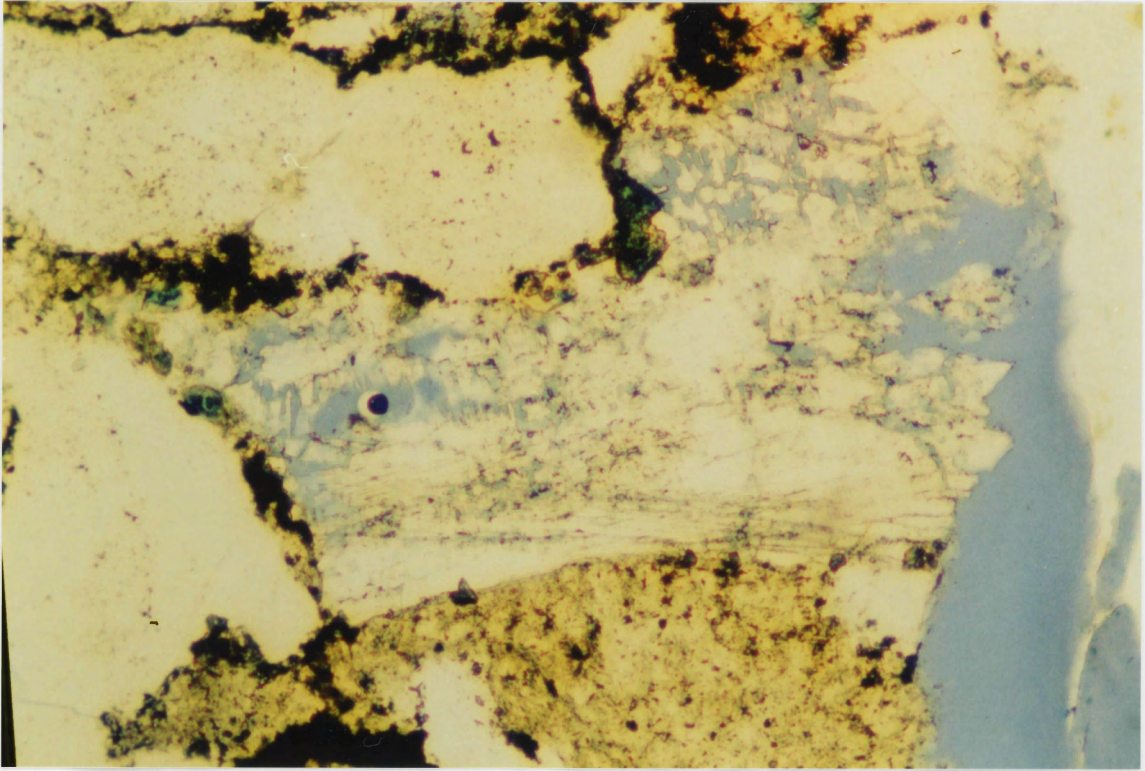
D
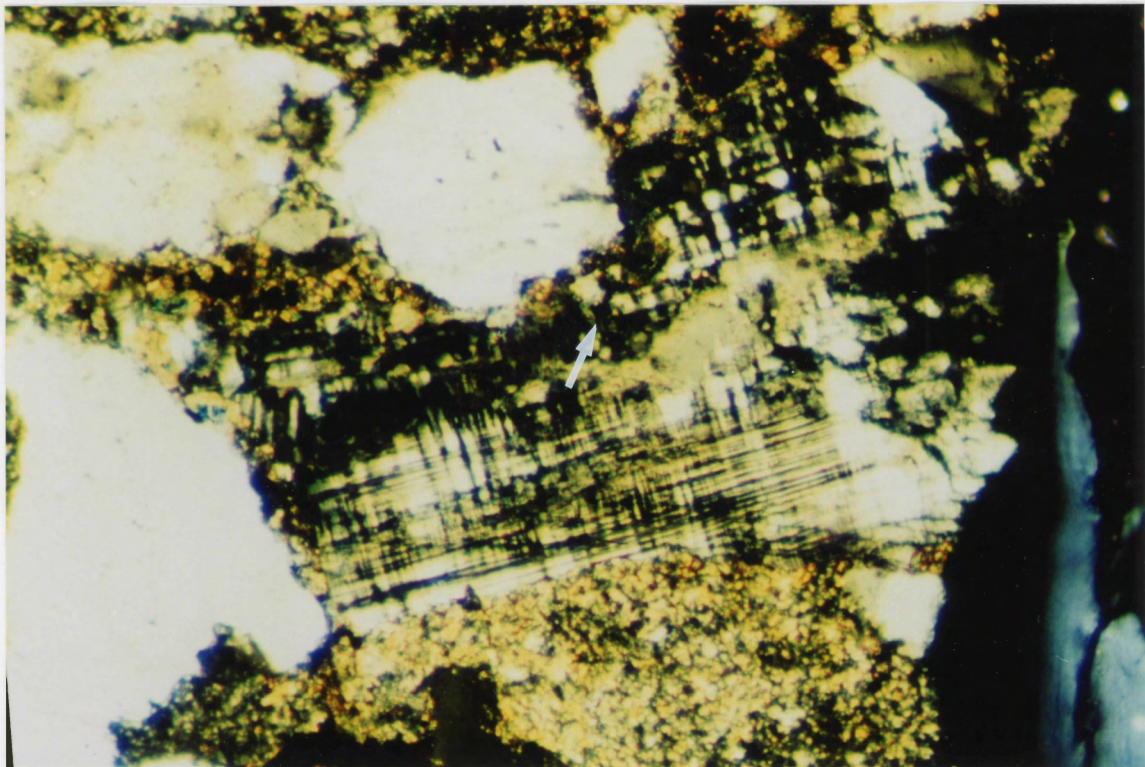
(C) Corroded microcline grain showing preferential dissolution along cleavages (blue) (magnification 64x, PPL). Quartz grains are rimmed with siderite. (D) Same as (C), but with crossed polars. Arrow indicates subhedral calcite crystals replacing feldspar.

pyrite, and minor tourmaline, hornblende and bone fragments. This group is relatively enriched in corroded feldspar, muscovite, siderite (cement and single grains) and lithic fragments compared to the previous three groups. Porosity is isolated in these samples, occurring mainly as intragranular porosity in the corroded feldspar grains. There is some intergranular porosity with associated kaolinite pore fillings. These rocks occur only at the base of PH250 (1,2, and 5). PH250-5 is probably transitional between this group and the fine-grained, low-porosity group but is most similar to the coarse-grained group.

3.2.5 Outburst Sandstones

The fifth group, sandstones that have actually outburst (OBT), includes three samples, one from Phalen (1994 outburst), one from #26 Colliery, and one from Merlebach Colliery. The petrology of these samples is quite similar to those in the coarse-grained low-porosity group, and they are placed in a separate group based only on their status as known outburst rocks. These sandstones are coarse-grained to small granule-size (average 1 mm), poorly sorted, poorly cemented, sub-mature litharenites (Figure 3.11). Quartz is subangular to subrounded monocrystalline and polycrystalline with highly sutured grains. Lithics are common and include subangular to subrounded metamorphic (schist) and igneous rock, quartzite, chert, clay/siltstone, and clay aggregates. Feldspar occurs most commonly as large, corroded grains with associated carbonate and kaolinite. Framework grains are in contact. Siderite commonly occurs as rims around framework grains, and has associated pyrite. The porosity of the outburst rocks is predominantly intragranular, within the cleavages of corroded potassium feldspar grains. Some intergranular porosity is present, and is associated with authigenic kaolinite and matrix clay patches. Permeability is quite low. Quartz grains in this group, as well as feldspars, typically
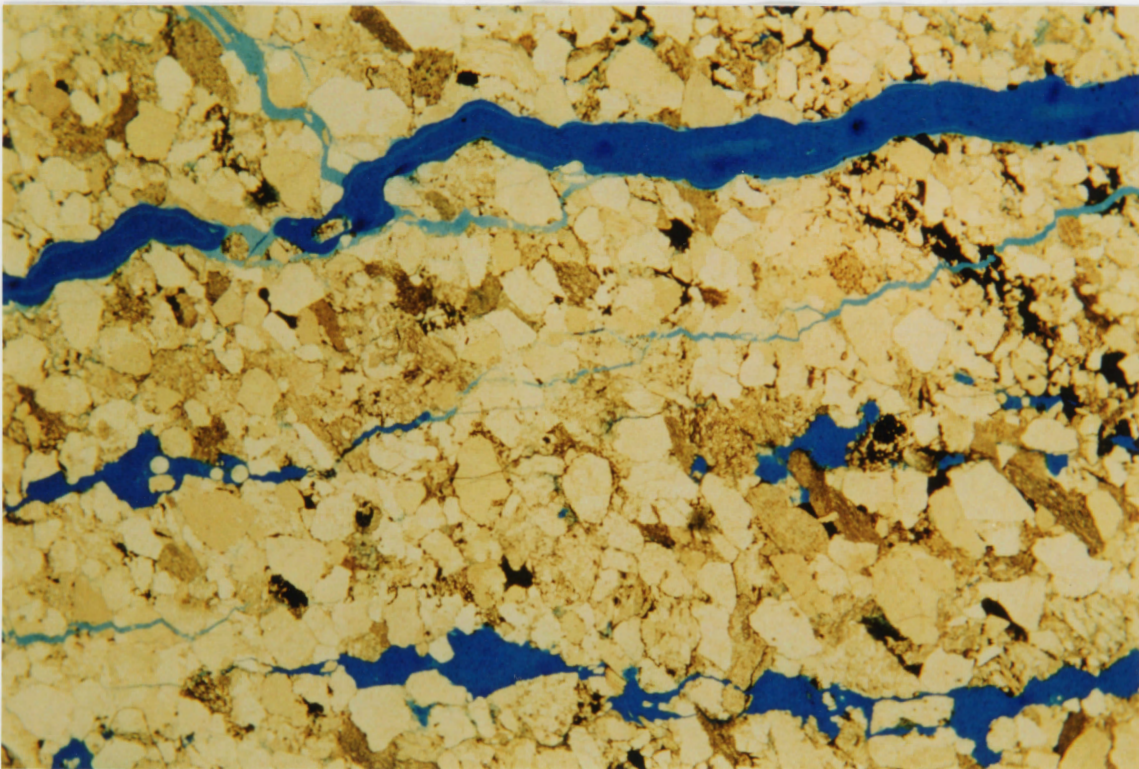
Figure 3.11 Example of OBT group (Phalen colliery). This is a coarse-grained, poorly sorted, sub-mature litharenite. Lithic grains are abundant, and porosity is low. Arrow indicates intragranular porosity in a corroded feldspar grain. Sub-parallel "lines" of blue are fractures forming "onion skin texture". The fractures formed due to the 1994 outburst (magnification 6.3x).

show fracturing of whole grains and "microcracks" within them. Hand specimens show a characteristic "onion-skin" texture (P. Cain, written communication, 1996). When the rocks outburst from the tunnel walls, they do so laterally, so that the fracture plane surface is parallel to the tunnel wall. These fractures commonly bisect individual grains, the two halves of which can be observed on either side of a fracture in thin section.

3.3.0 Clay and Pore Morphology

The environmental scanning electron microscope was used to determine structure and composition of clays and other cements in the outburst sandstones, and to closely examine pore morphology. Figure 3.12 shows ESEM images of distinctive kaolinite "books" that occur as pore fillings in several of the outburst sandstones. Analyses made using the EDS detector confirmed that this particular clay is kaolinite. The ESEM images also reveal the extremely low porosity of these sandstones, which is due largely to intergranular clay (Figure 3.13). Most quartz grains, which make up a significant portion of almost all of the samples, are coated in what appears to be a layer of clay, which in turn may be coated in a second, later generation of clay such as kaolinite. Corroded feldspars (Figure 3.14) and fractured quartz grains from outbursts (Figures 3.15) were also examined with the ESEM. The images of the corroded feldspar clearly show preferential dissolution along cleavages and cleavage intersections and at grain boundaries. Dissolution begins as small pits arranged in a linear fashion. As the pits enlarge, they join together, and eventually the entire grain will be corroded and/or replaced. Rocks from groups CGLP (coarse-grained, low porosity) and OBT (outburst samples) were compared using the ESEM and are very similar morphologically, with the exception of highly fractured quartz grains, which do not occur in the coarse-grained low-porosity group (CGLP).

A
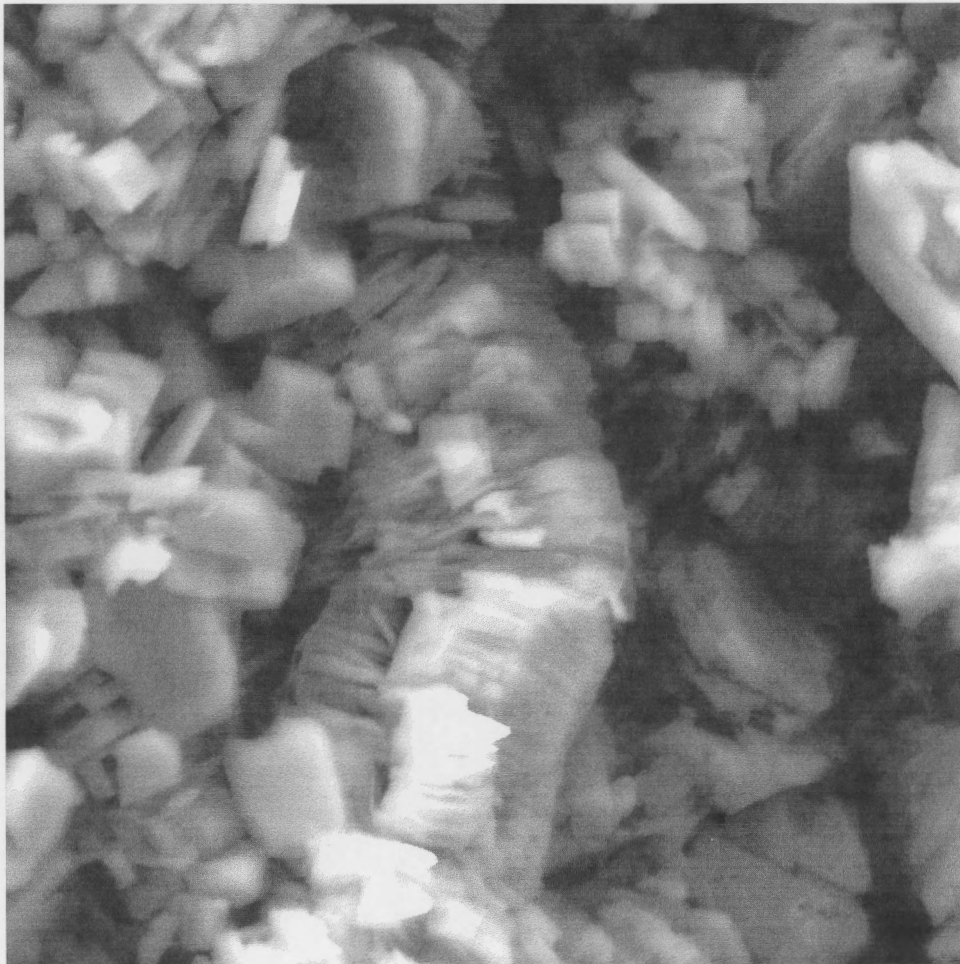
10 μm

Figure 3.12 ESEM image of pore-filling kaolinite books.
(A) Pseudohexagonal kaolinite occurring in vermicular
"books" as a pore-filling mineral, from 250-3 (CGLP).

B
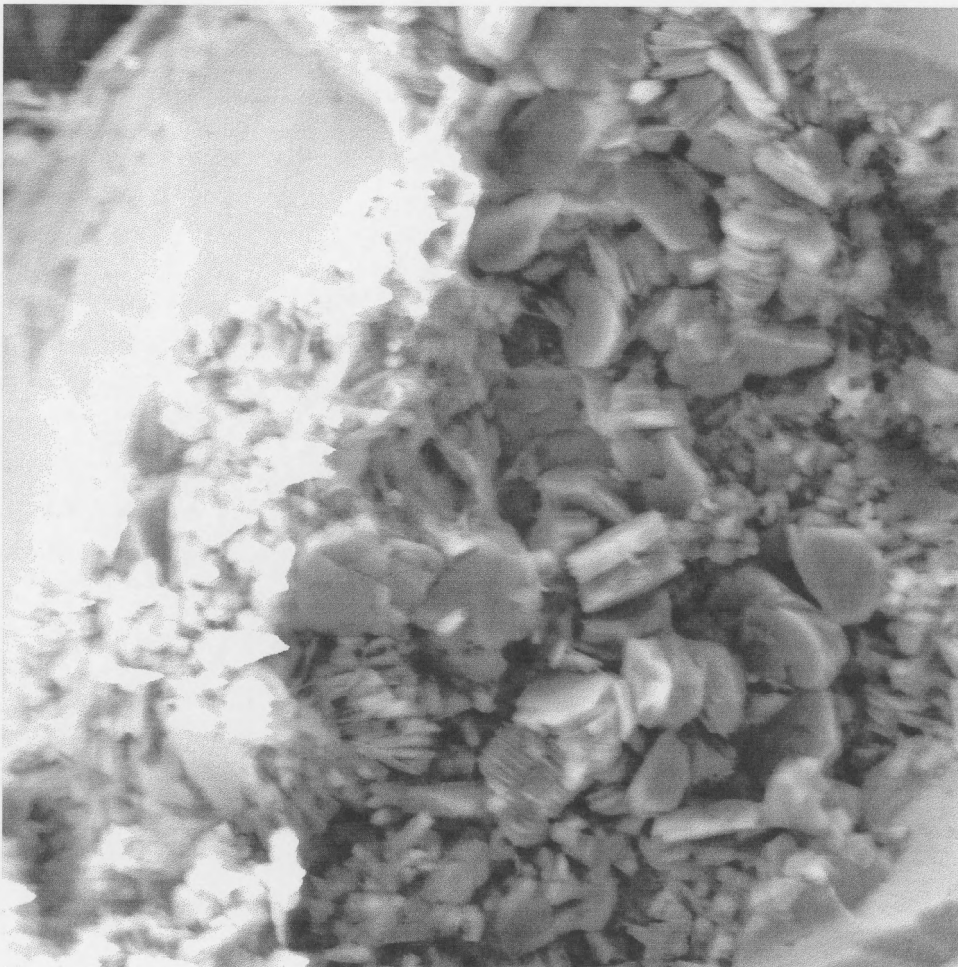
20 μm

(B) Kaolinite books filling porosity between quartz grains. Sample is from the 1994 Phalen outburst.
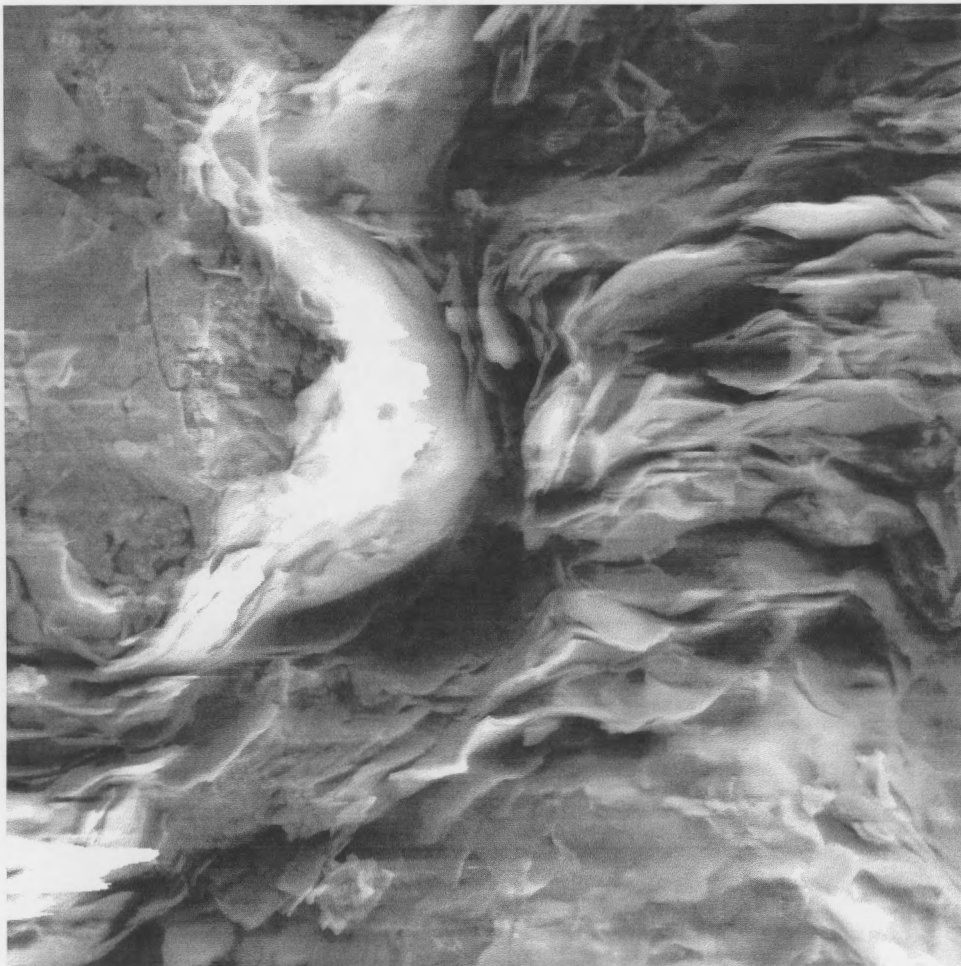
50 μm

Figure 3.13 ESEM image of intergranular clay (illite?). It is compacted between two quartz grains (upper left and lower right corners).

A
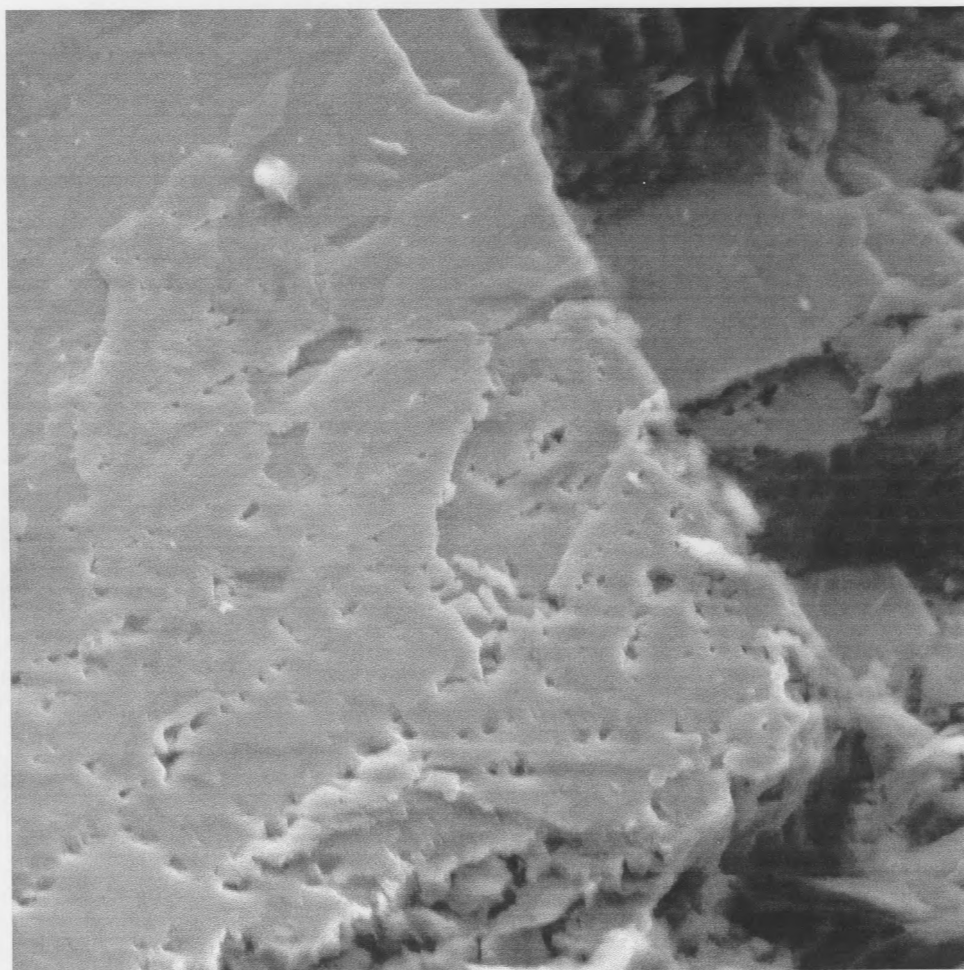
20 μm

Figure 3.14 ESEM images of corroded feldspar. (A) Corner of a feldspar grain showing early dissolution. Dissolution begins as small pits that eventually enlarge and join to form cleavage-parallel porosity.

B
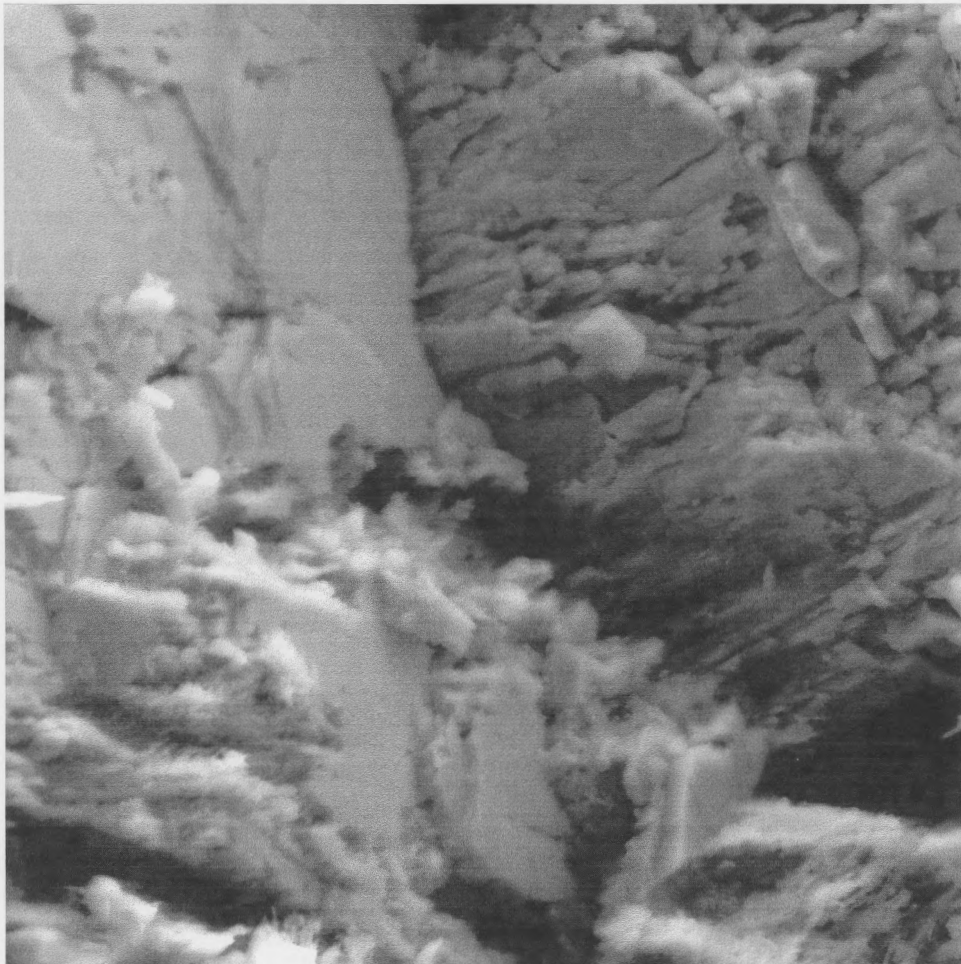
20 μm

(B) Feldspar grain showing well-developed preferential dissolution along cleavage planes and intersections. Texture appears somewhat skeletal.
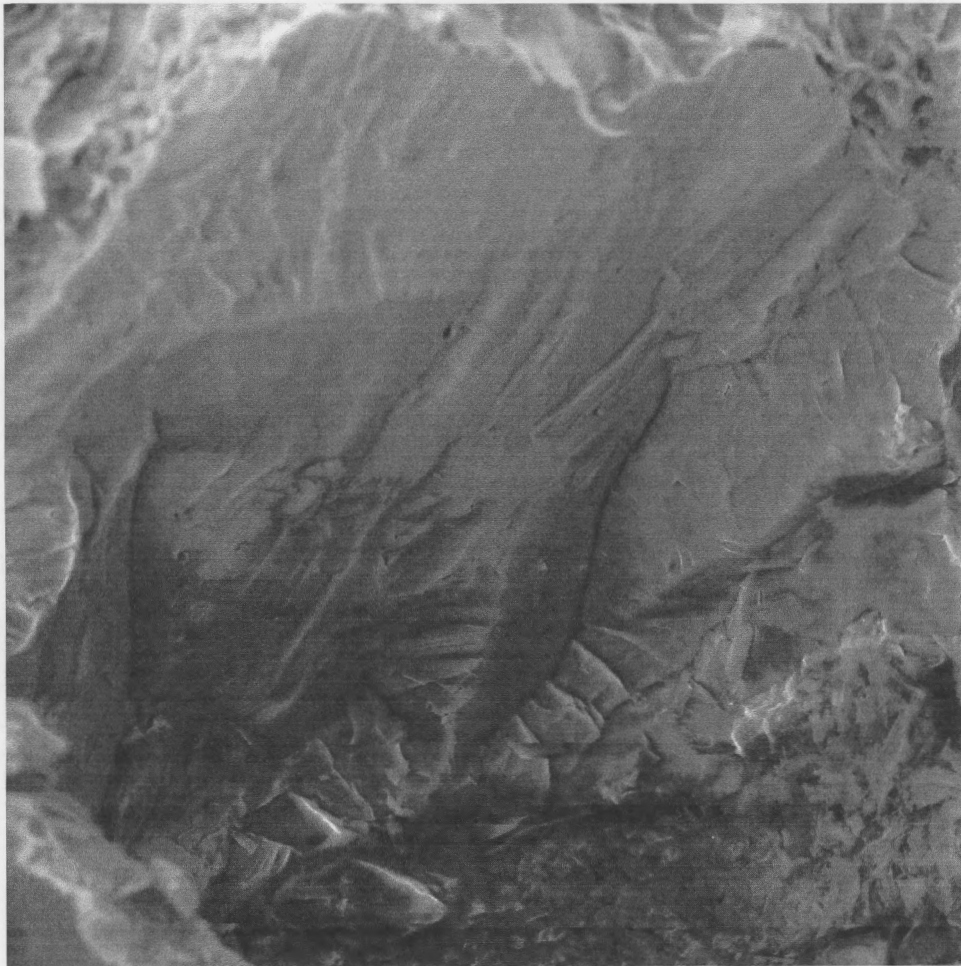
50 μm

Figure 3.15 ESEM image showing a fractured quartz grain in an outburst sandstone (Phalen). Non-outburst quartz does not show this texture. There is intergranular clay occurring in the lower right corner of the image.

3.4.0 Feldspar Composition

Several corroded feldspar grains were analyzed with the electron microprobe in order to

determine if they were calcic, sodic, or potassic in nature. This was not possible in thin section

due to the extremely degraded state of the grains and general absence of crystal twins. Results

show that the corroded feldspars are potassium rich, while the smaller, non-corroded feldspars are

albitic. Knowing the composition of the feldspars is important for determining some of the

reactions that might have taken place in the rock during diagenesis, for example the formation of

kaolinite, and calcite overgrowths within feldspar. Microprobe results appears in Appendix D.

3.5.0 Porosity and Permeability

3.5.1 Porosity

Density of the complete Phalen cores was determined using the Multi-Sensor core logger

(MST). The density logs obtained from the MST can be converted to porosity logs using bulk

and grain density measurements from samples of the core, but due to calibration difficulties, the

MST porosity is not available for the thesis. The density curves are relatively, but not absolutely

accurate, and the curve should be shifted to the left or right to match with measured density

values obtained through directly measuring bulk density. Trends in density, however, correlate

well with the major units shown in the stratigraphic logs (PH-250, Figure 3.16; PH-102, 3.17).

Porosity values obtained from the MST can be verified by comparing them to values

obtained by AGAT Laboratories (Table 3.1). AGAT porosity values are not available for the

samples of rock that have actually outburst (OBST, M-1, PHUN). Measured porosity for PH-

250 ranges from 4.5% to 7.7% (mean 6.5%). For PH-102 the values are slightly higher, ranging

from 6.9% to 12.1% (mean 8.5%). Figure 3.18 shows a graphical representation of porosity for
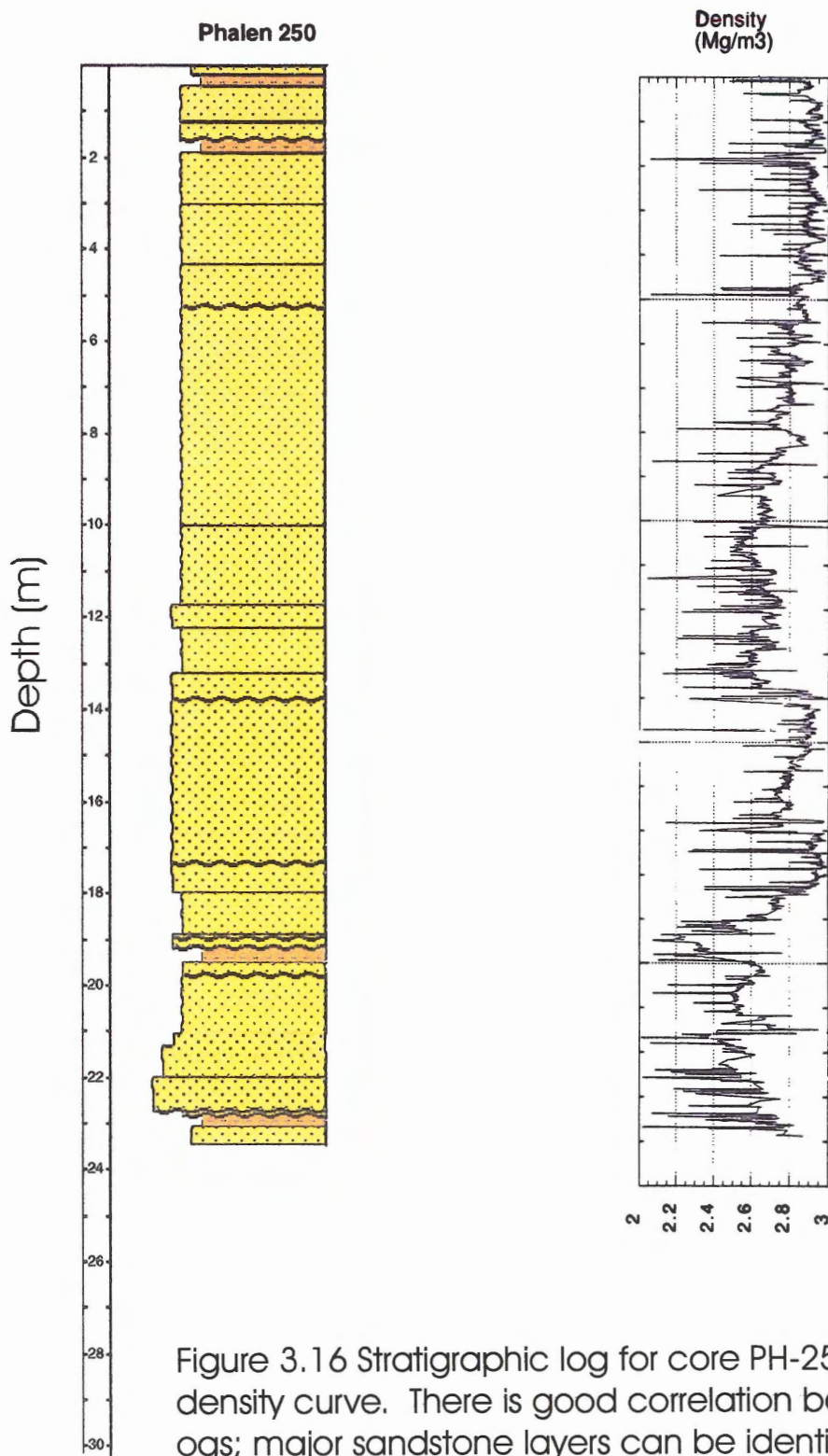
Figure 3.16 Stratigraphic log for core PH-250 with MST density curve. There is good correlation between these ogs; major sandstone layers can be identified. Note that the density values are relatively, but not absolutely, correct. The values must be shifted left or right after calibrations are completed. See Figure 3.2 for legend.

Phalen 102

Depth (m)
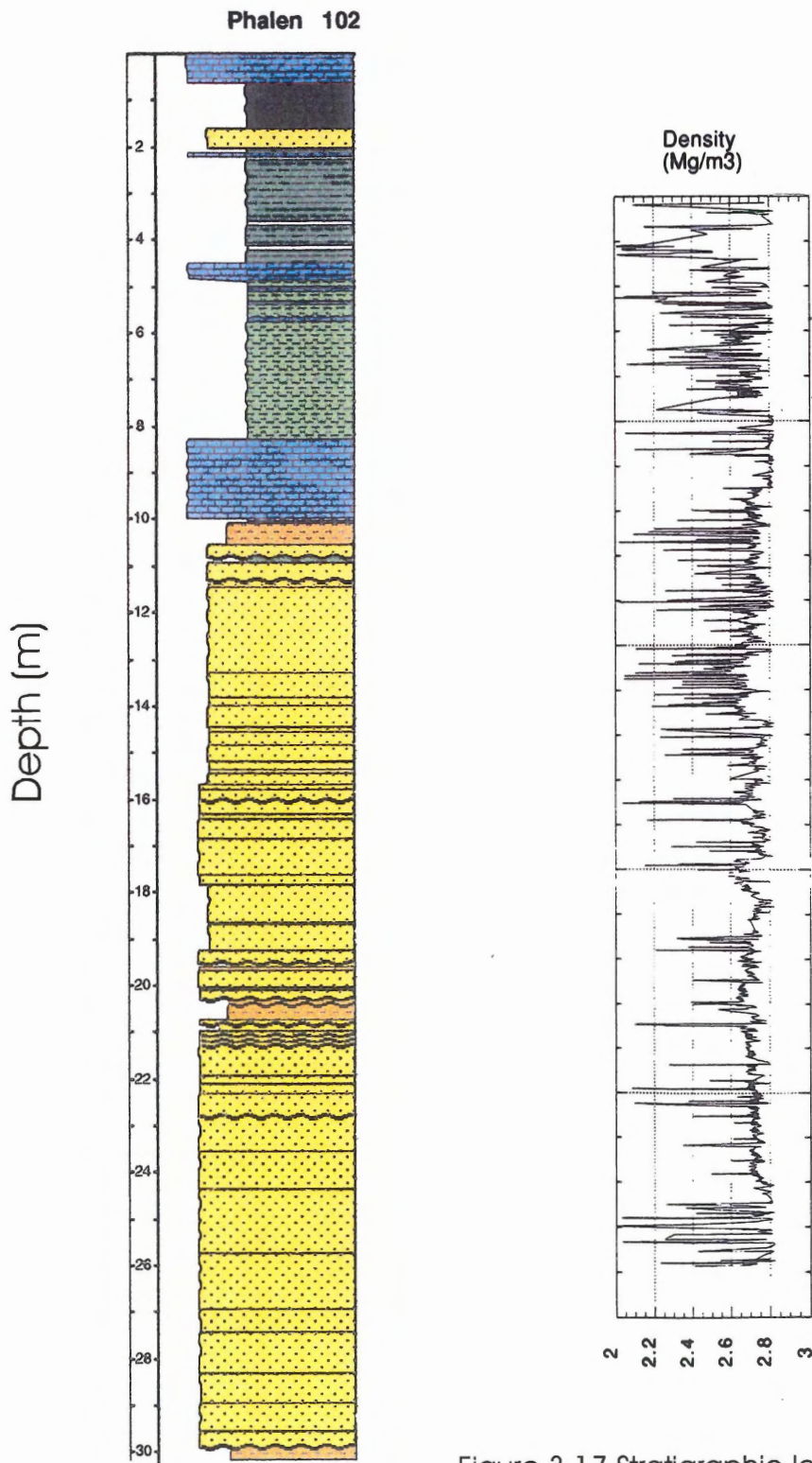
Density
(Mg/m3)

Figure 3.17 Stratigraphic log for core PH-102 with MST density curve. There is good correlation between these logs. Major sandstone layers can be identified. The top 6 m of core did not provide useful density data. See Figure 3.3 for legend.

Table 3.1 Porosity data for all sandstone samples from PH250 and PH102 analyzed by AGAT Laboratories.

Sample NO.	Petrographic Group	Porosity	Sample NO.	Petrographic Group	Porosity
250-1	CGLP	0.064	102-1	LAG	0.080
250-2	N/A	0.062	102-3	FGHP	0.080
250-3	CGLP	0.065	102-5	LAG	0.121
250-4	N/A	0.077	102-6	FGHP	0.079
250-5	CGLP	0.059	102-9	FGHP	0.082
250-6	FGLP	0.058	102-11	FGHP	0.083
250-7	N/A	0.077	102-12	FGHP	0.083
250-8	N/A	0.063	102-13	FGLP	0.069
250-9	N/A	0.066			
250-10	LAG	0.063			
250-11	N/A	0.045			
250-12	FGLP	0.070			
250-13	N/A	0.075			
250-14	N/A	0.065			
250-15	FGLP	0.066			
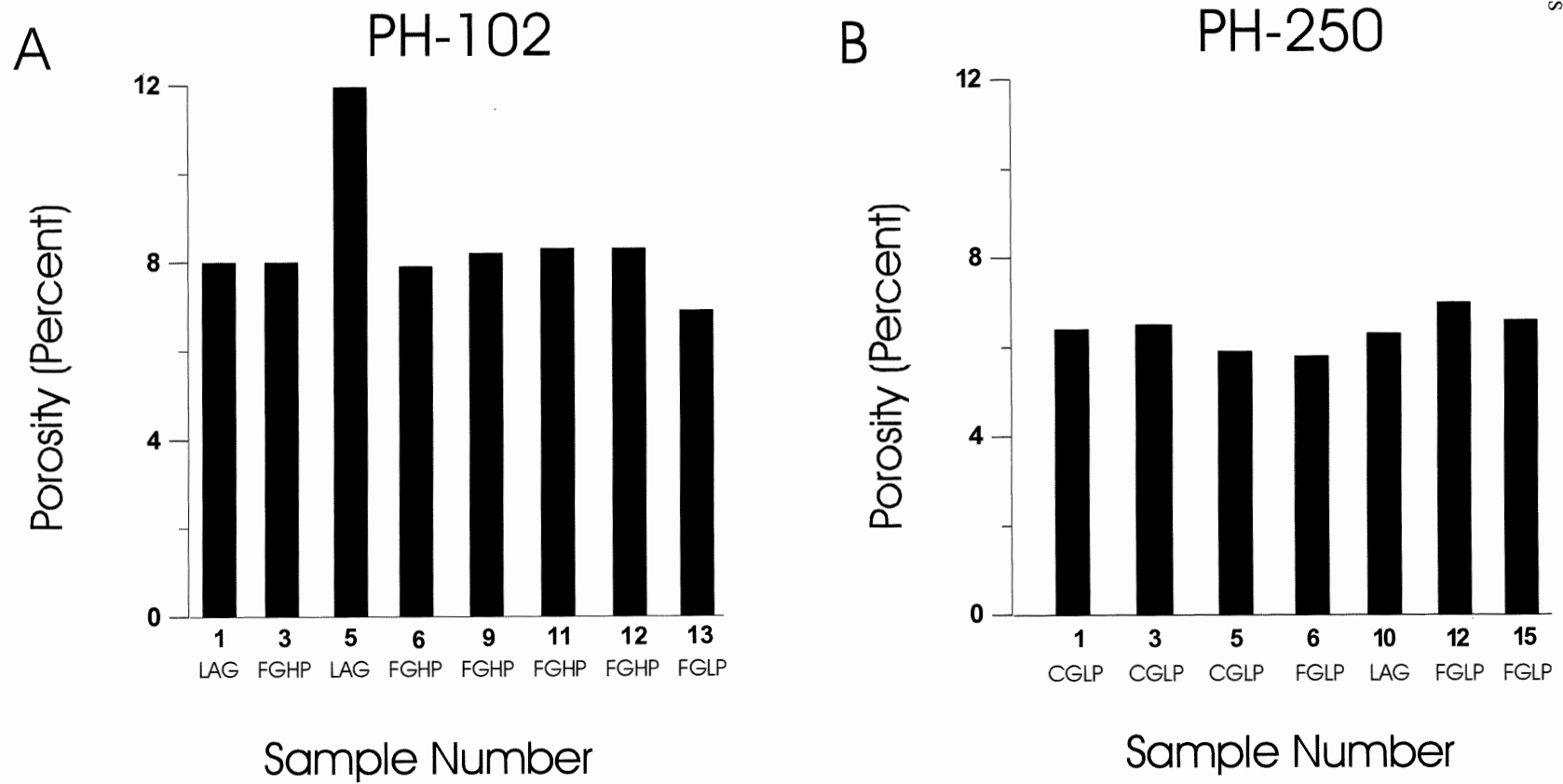
Figure 3.18 Graph of porosity for Phalen cores. (A) PH-102. There is some variability through the core. (B) PH-250. There is less variability in this core than in PH-102.

PH-250 and PH-102. Figure 3.19 shows the same data as 3.18, but the samples have been

grouped according to the petrographic groups defined earlier, and not by stratigraphic position

within their respective cores. It is important to note that porosity and permeability data were

measured from the same stubs used to make the thin sections used in the petrographic

descriptions, which allows for good comparison of the data sets.

3.5.2 Permeability

Permeability values for the two cores were obtained from AGAT Laboratories (Table 3.2).

Horizontal permeability (K_{max}) for PH-250 ranges from less than 0.01 to 0.19 millidarcies. For

PH-102 values range from 0.03 to 3.02 millidarcies. No permeability values are available for the

actual outburst samples. Permeability values for the two Phalen cores are summarized in Table

3.2. Permeability of PH-250 generally decreases up section, whereas PH-102 shows the opposite

trend, with the highest permeability occurring in the stratigraphically highest samples, with the

exception of PH102-5, which represents a lag deposit. This is presented graphically in Figure

3.20. Figure 3.21 shows the same data as 3.20, but the samples have been grouped according to

the petrographic groups defined earlier, and not by stratigraphic position within their respective

cores.
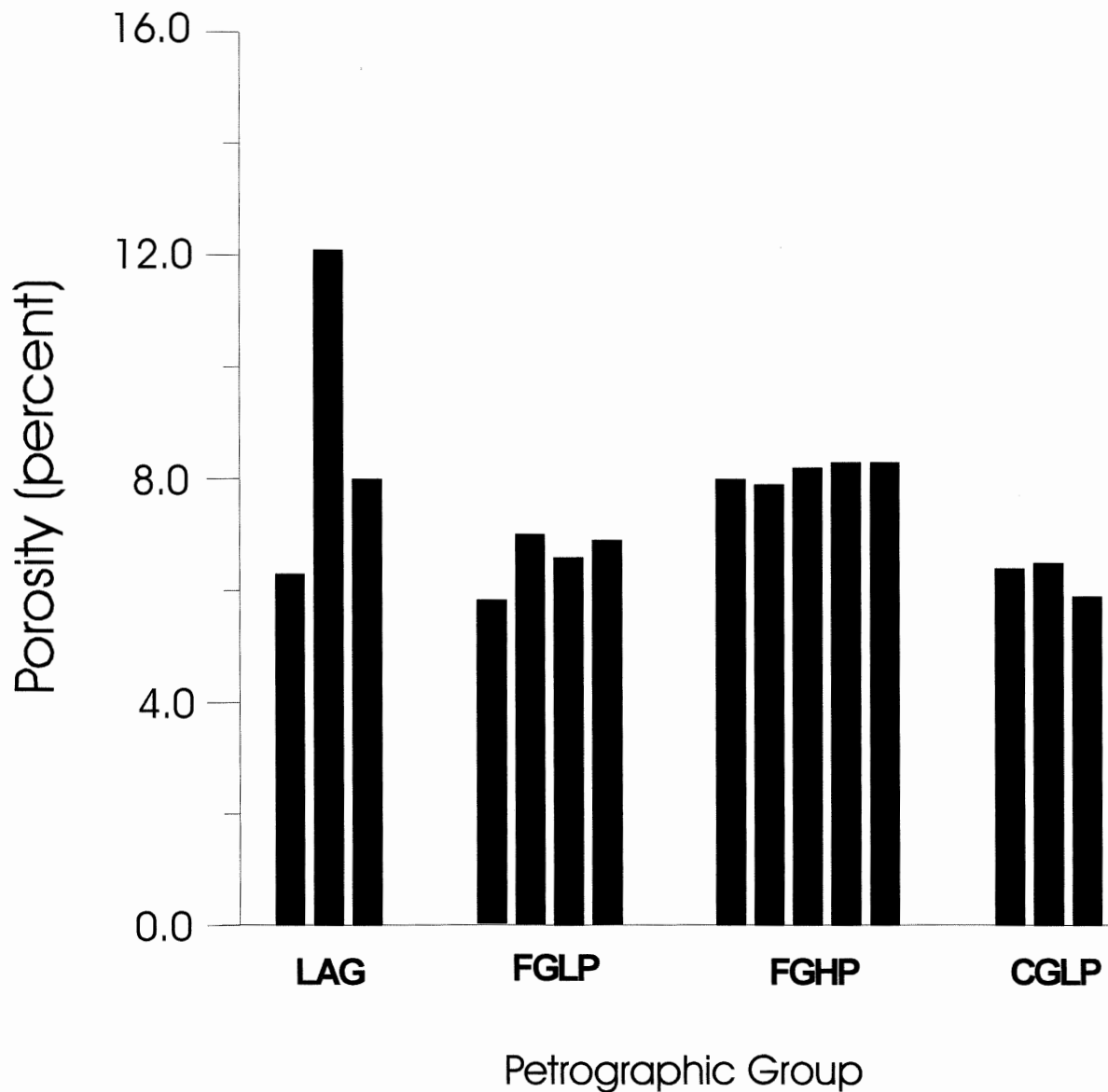
Figure 3.19 Porosity of Phalen channel sandstones by petrographic group. No numerical data was available for the outburst sandstones (OBT).

Table 3.2 Permeability data for all sandstone samples from PH250 and PH102 analyzed by AGAT Laboratories.

Sample NO.	Petrographic Group	K_{max} (mD)	Sample NO.	Petrographic Group	K_{max} (mD)
250-1	CGLP	0.06	102-1	LAG	0.030
250-2	N/A	0.06	102-3	FGHP	0.050
250-3	CGLP	0.08	102-5	LAG	2.540
250-4	N/A	0.19	102-6	FGHP	0.110
250-5	CGLP	0.04	102-9	FGHP	0.110
250-6	FGLP	0.03	102-11	FGHP	0.300
250-7	N/A	0.05	102-12	FGHP	0.910
250-8	N/A	0.03	102-13	FGLP	3.020
250-9	N/A	0.05			
250-10	LAG	0.02			
250-11	N/A	<0.01			
250-12	FGLP	0.05			
250-13	N/A	0.04			
250-14	N/A	0.04			
250-15	FGLP	0.02			
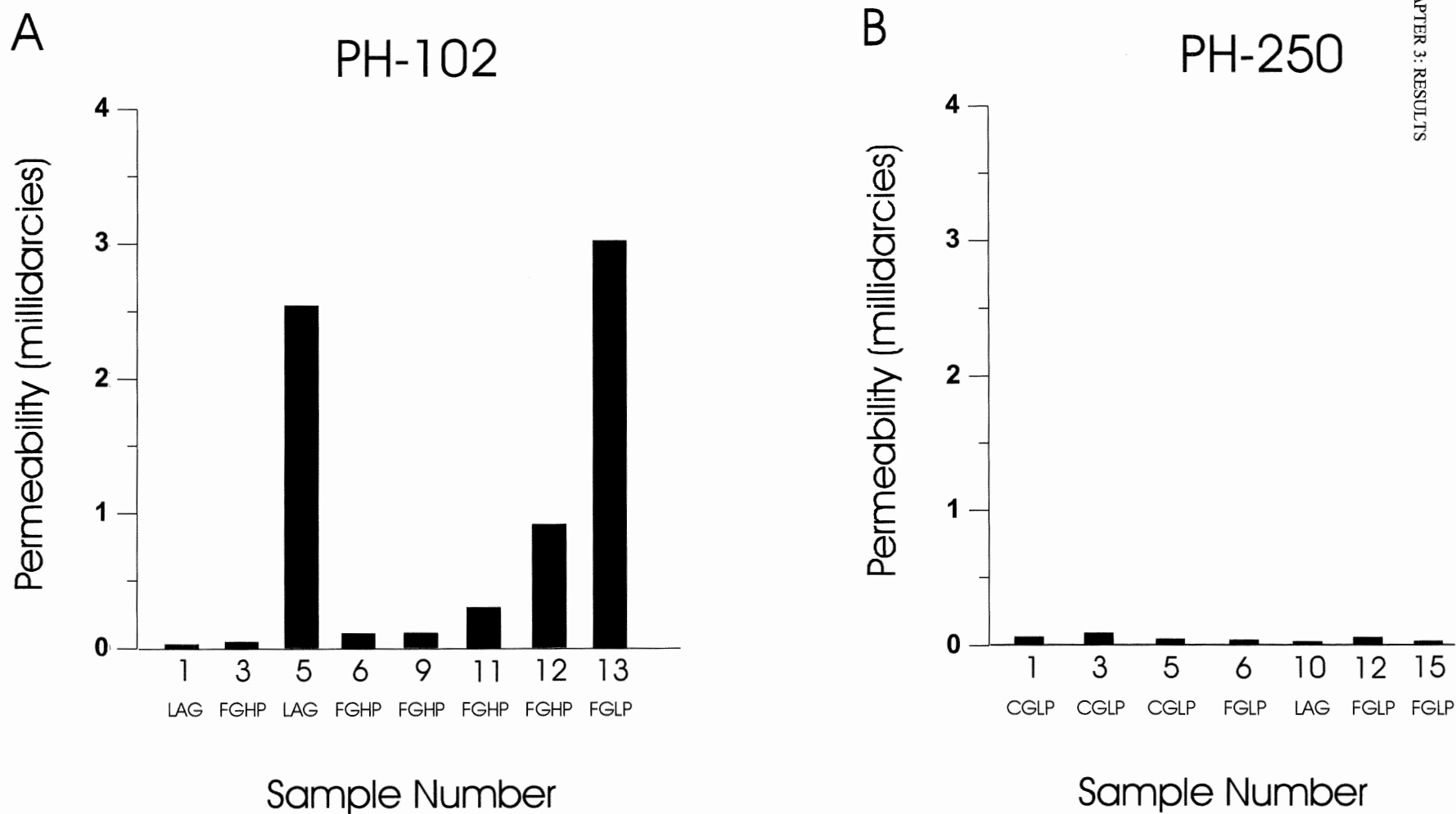
Figure 3.20 Graph of permeability Phalen cores. (A) PH-102. Permeability values are greatest at the stratigraphically highest section of the core. (B) PH-250. Permeability is greatest at the stratigraphically lowest section of core.
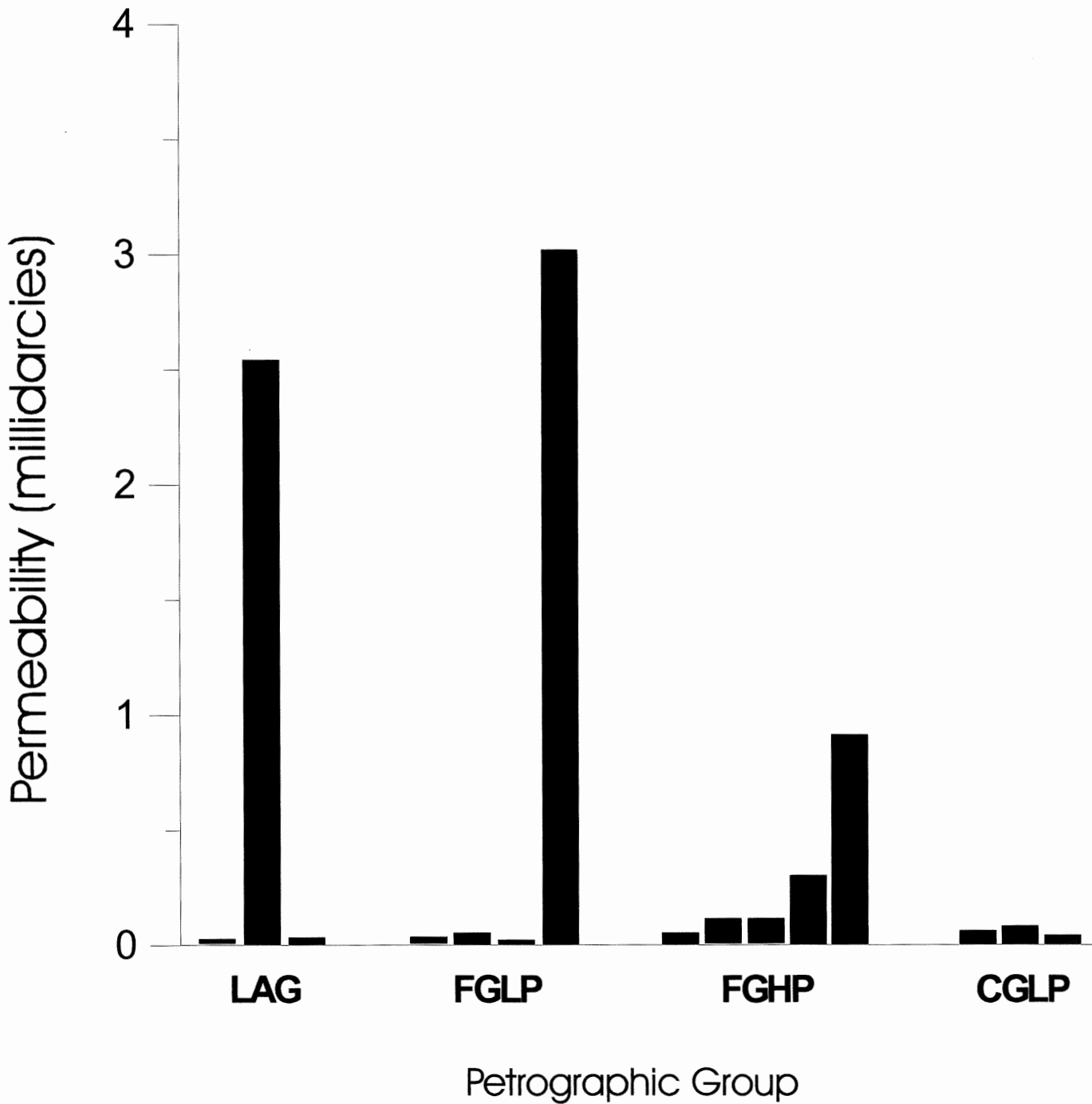
Figure 3.21 Permeability of Phalen channel sandstones by petrographic group. No numerical data was available for the outburst sandstones (OBT).

Chapter 4 Discussion

4.1.0 Introduction

The objective of this study is to characterize the outburst channel sandstones of the Phalen Colliery through analysis of petrography, porosity, and permeability. Thin section work reveals differences in detailed petrography both within and between PH-102 and PH-250. Similar trends occur for porosity and permeability. By comparing PH-102 and PH-250 to samples of actual outburst rock, one can infer relationships between petrography, porosity and permeability, and outburst risk. Some characteristics of the outburst rocks might be used in Phalen, or other mines, as partial indicators of increased outburst risk.

4.2.0 Petrography and Outburst Potential

4.2.1 Compaction of Lithic Grains

The abundance of lithic fragments varies significantly across the five petrographic groups discussed in Chapter 3 (Figure 4.1). Lithic grains are most common in the coarse-grained low-porosity rocks (14.6%) and in the outburst rocks (10.3%); lithic fragments are smaller and less common in LAG (6.7%), FGLP (5.1%), and FGHP (5.4%). The submature rocks (CGLP, OBT) had the greatest variety in lithologies (sedimentary, igneous, metamorphic), whereas the finer-grained rocks tended to have more clay/siltstone clasts. LAG group has intraformational claystone and siderite clasts.

The compaction of lithic fragments greatly affects the amount of porosity present in a sandstone. In CGLP and OBT, the lithics are commonly contorted, deformed, and "wrapped" around relatively rigid quartz grains (Figure 4.2). This compaction has led to a decrease in intergranular porosity. Some lithics are so compressed they can only be distinguished from
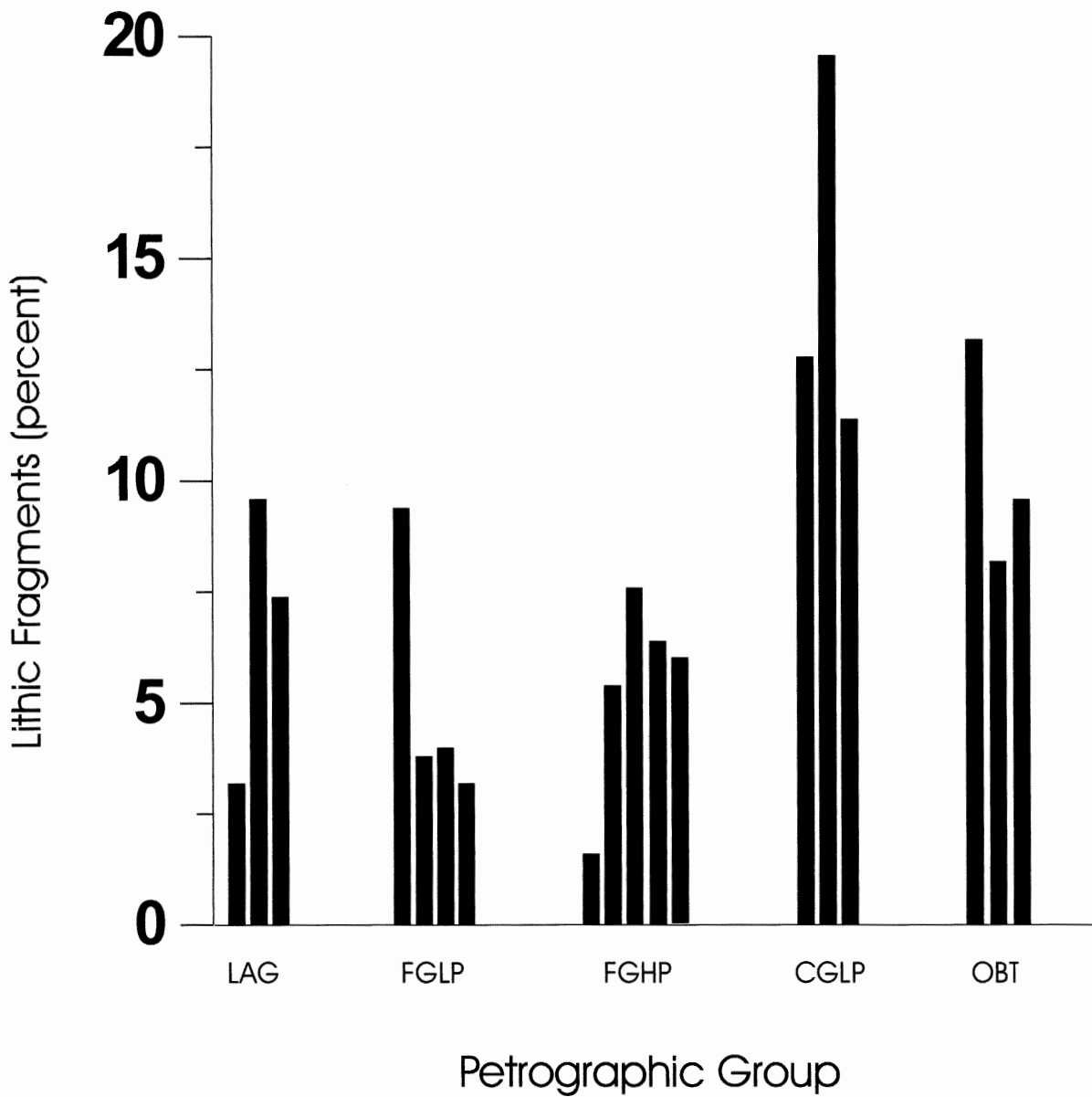
Figure 4.1 Percent lithic fragments by petrographic group.
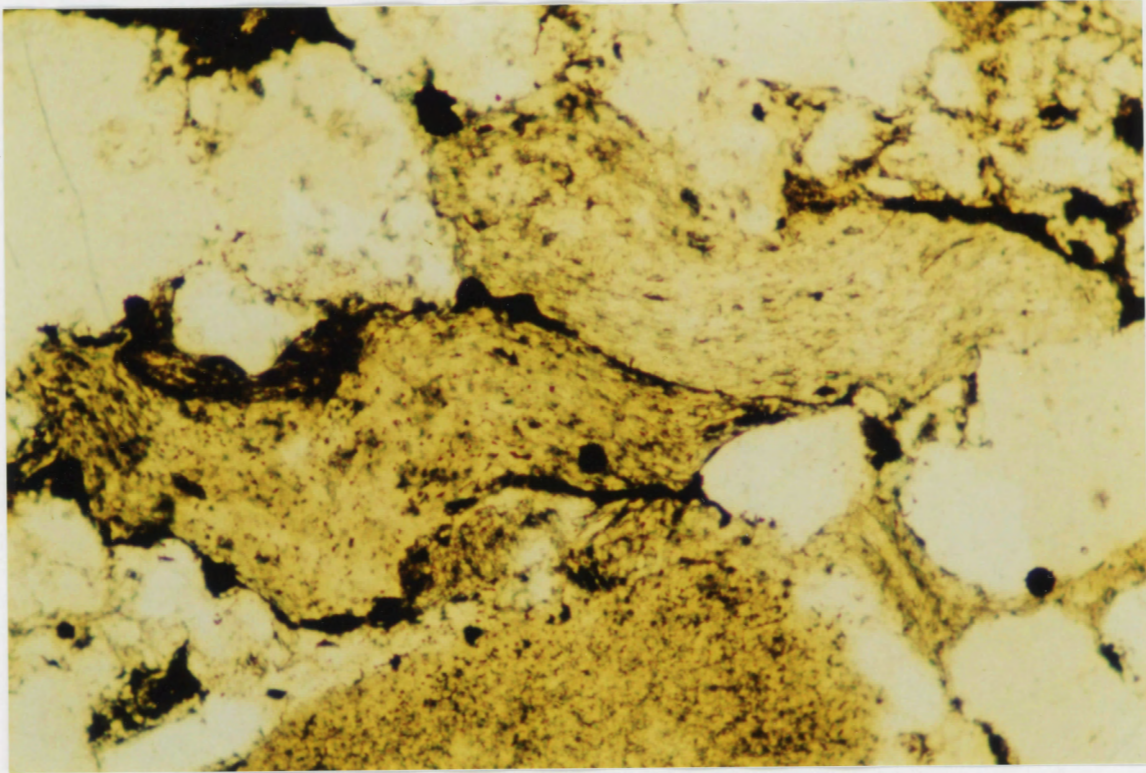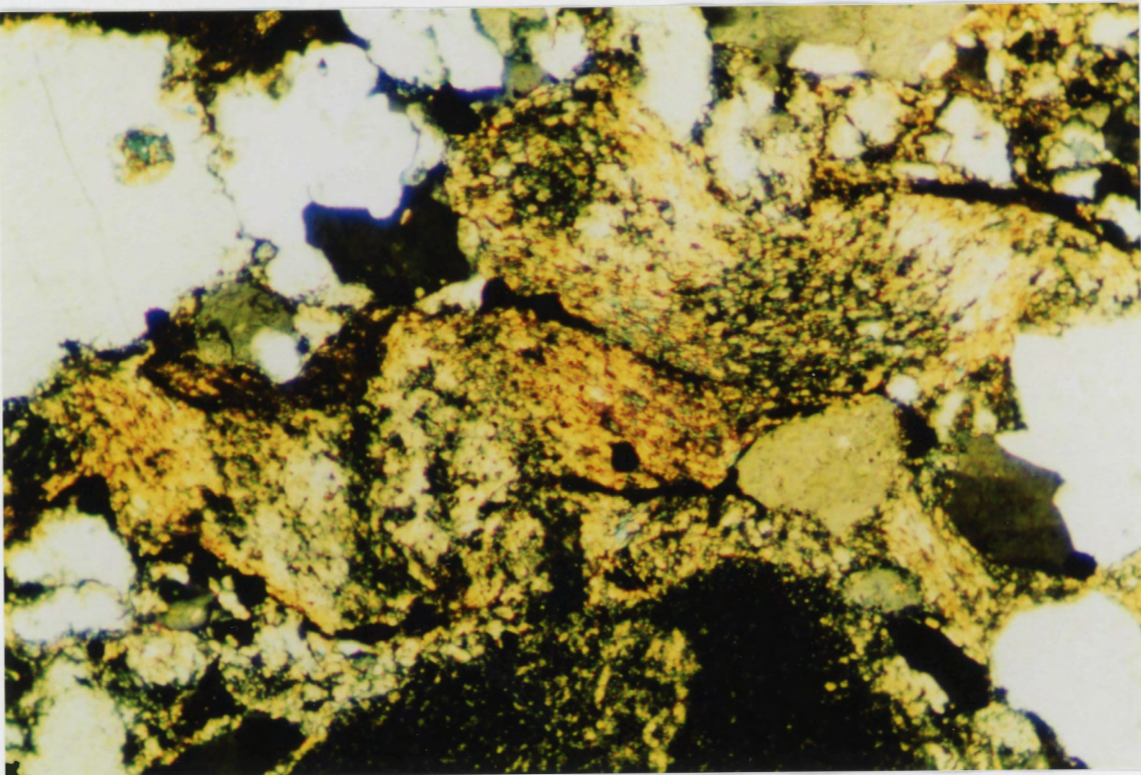
Figure 4.2 (A) Lithic grains. They were deformed by early mechanical compaction. Note the indentation by relatively rigid quartz grains. Grains are rimmed by siderite (magnification 64x). (B) Same as (A), but with crossed polars. Note the deformed fabric defined by aligned clay minerals.

pore-filling matrix based on subtle clay mineral alignment. In the finer grained rocks the

"wrapping around" effect does not occur because the lithic grains tend to be the same size as the

other framework grains, but there is evidence of lithic deformation. The lithic grains in FGHP and

FGLP are commonly "squeezed" into pore spaces, reducing primary porosity. Lithic compaction

was one of the first events to occur in the diagenetic history of these sandstones, during early

burial. This is known from relationship between cements (siderite, calcite) and lithic grains.

There were evidently abundant pore spaces for the lithic grains to be "squeezed" in to, which

implies that cements probably were minor or not yet deposited.

The compaction of lithic fragments not only fills pore spaces between the framework

grains, but also results in a decrease in permeability due to the blocking of pore throats that

connect intergranular porosity. Lithic compaction also serves to further isolate intragranular

porosity that is present within the corroded feldspars. As mentioned previously, restricted

permeability is one of the key factors that has been associated with outburst risk. The compaction

of lithics clearly provides a mechanism of permeability and porosity reduction.

4.2.2 Corrosion of Feldspar

Corroded feldspar content varies significantly between the five petrographic groups

(Figure 4.3). It was encountered in all of the outburst rocks studied (OBT - 4%) and in the

immature basal section of PH-250 (CGLP - 3.1%). In the fine-grained rocks (FGLP, FGHP) and

lag deposits (LAG) the corroded feldspar content was less than 0.5%.

The corrosion of potassium feldspar grains provides an important source of isolated

intragranular porosity within PH-250 and the outburst rocks. The corroded feldspars provide an

effective stratigraphic trap for gas because the grains act as a gas storage area, but the low bulk
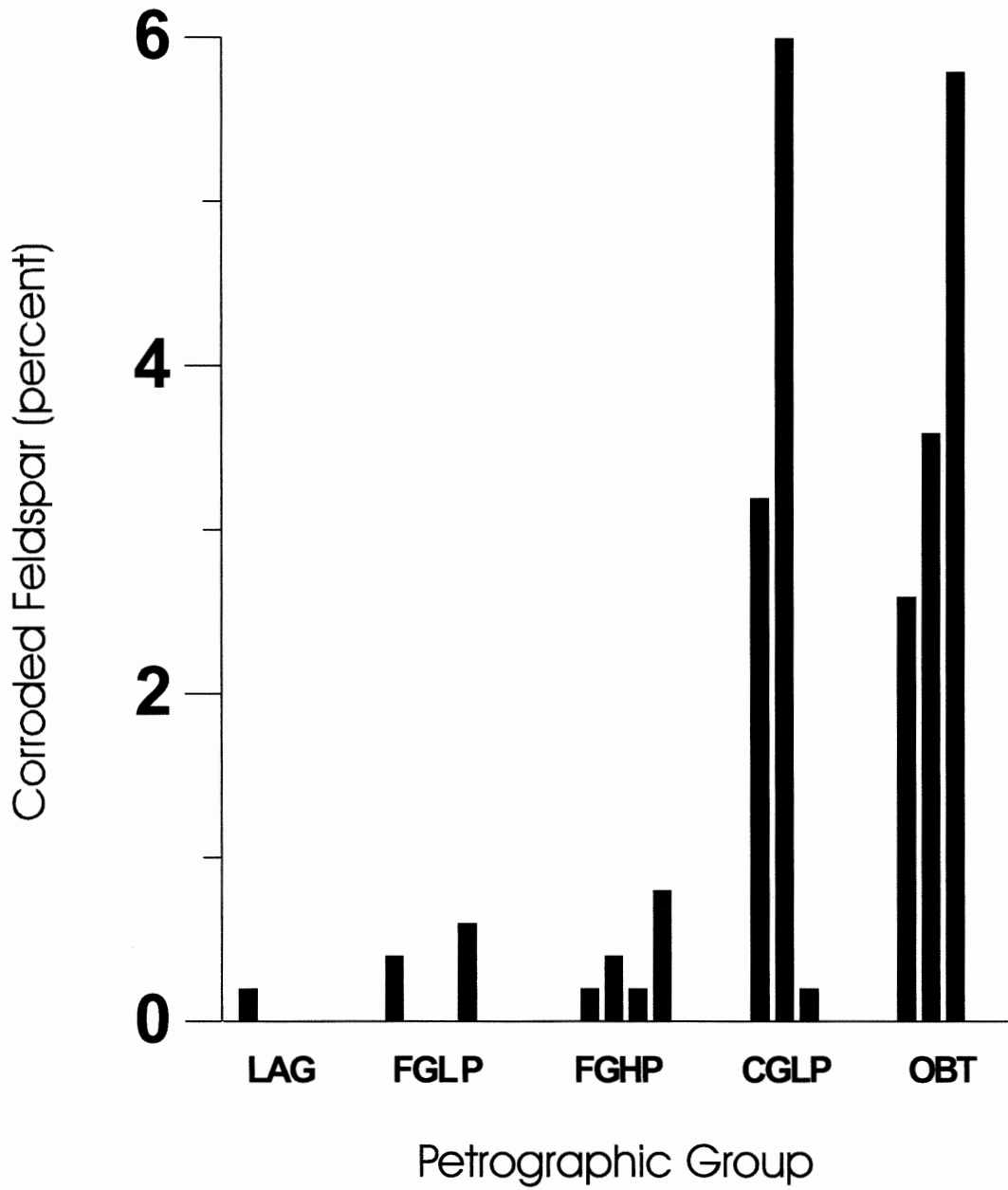
Figure 4.3 Percent corroded feldspar by petrographic group.

permeability of these rocks should prevent the gas from escaping.   This results in an increase in

outburst potential. In the fine grained rocks and lag deposits, which lack corroded feldspar,

porosity is predominantly intergranular with relatively good permeability. Any spaces in which

gas could be trapped are somewhat connected, allowing for some degree of gas movement

through the rock (both naturally and during mine operations). Poorly sorted, submature rocks are

more likely to have large grains of corroded feldspar, which permit isolated gas storage, but

restrict permeability, increasing the risk of a gas explosion.

4.2.3 Kaolinite Content

Kaolinite commonly occurs as a pore-filling mineral in PH-102 (FGHP) and comprises on

average 10.6% of the rock (Figure 4.4). Kaolinite is less common in the immature sandstones of

basal PH-250 (CGLP - 5.8%) and the outburst samples (OBT - 5.7%). In CGLP and OBT

samples, kaolinite is typically associated with corroded potassium feldspar as a replacement

mineral or with rare to occasional intergranular porosity. Kaolinite comprises, on average, only

1.7% of the lag samples, and 1.25% of the fine-grained, low porosity samples. Figure 4.5 shows

the distribution of kaolinite across the five petrographic groups. This graph emphasizes the

similarity between the outburst rocks and those occurring at the base of core PH-250 (CGHP). It

also highlights the abundance of kaolinite in PH-102 (FGHP group).

The distribution of kaolinite is inferred to be an important factor in outburst potential, and

could be used as an indicator of this risk. When kaolinite is evenly distributed through the rock, it

is associated with relatively high permeability and slightly higher than average porosity values. In

the rocks that show lower but still significant amounts of kaolinite (CGLP, OBT) the porosity is

isolated, and consequently permeability is lower, resulting in a decreased capacity for gas escape.
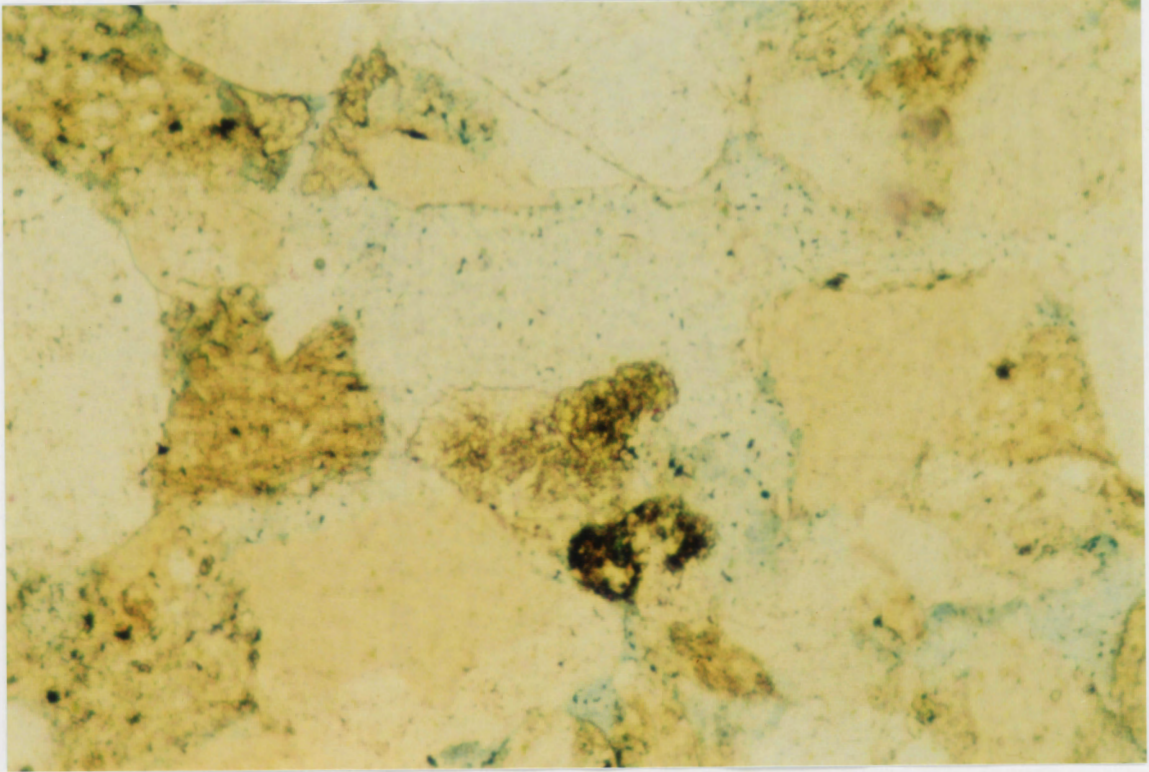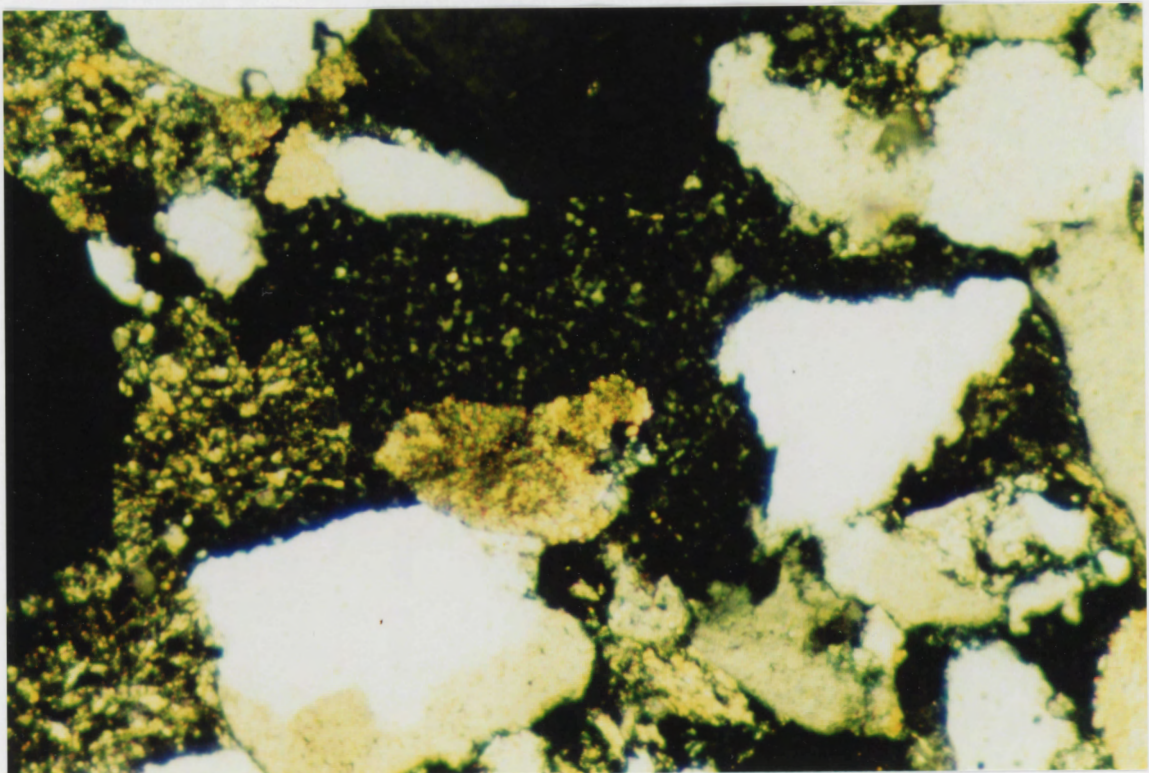
Figure 4.4 (A) Example of intergranular porosity and pore-filling kaolinite from FGHP group (blue areas). Permeability is relatively good (magnification 64x). (B) Same as (A), but with crossed polars.
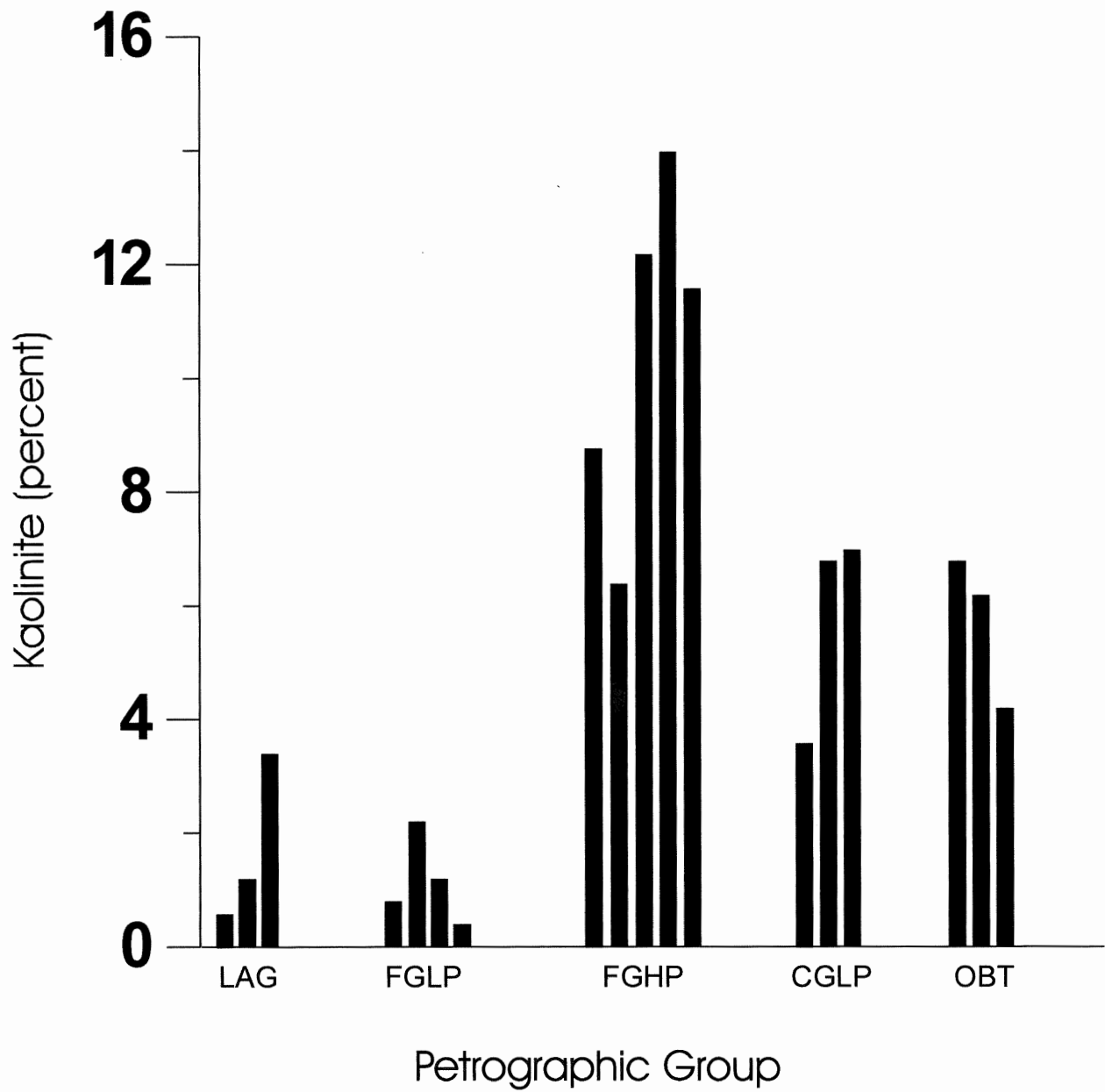
Figure 4.5 Percent kaolinite by petrographic group.

Again, this decrease in permeability will contribute to increasing outburst potential. The mobility of individual flakes from kaolinite books may contribute to reductions in permeability if there is groundwater flow (through pore-throat clogging).

4.3.0 Controls on Sandstone Petrology

4.3.1 Controls on Lithic Grain Distribution

Important controls on the distribution of lithic grains within the Phalen rocks include source, transport, and sorting. It is possible that the submature rocks in CGLP have a different source area than the fine-grained rocks in FGLP and FGHP, for example granitic fragments versus a recycled sandstone, however the source area for the channel sandstones is unknown. Transport distance might also be responsible for the differences in lithic distribution, as it affects sorting, abrasion, and chemical weathering. Metamorphic quartz, for example, is most common in CGLP, and might not normally survive extended transportation. The framework grains in FGLP and FGHP are somewhat more rounded than in CGLP, OBT, and LAG, and the lithic grains are smaller. This could be explained by longer transport sorting and abrasion. Diagenesis would probably not have a large effect on the distribution of lithic fragments. More important is the degree of deformation they experience due to early compaction. Some lithic fragments show alteration to clay, which could affect the porosity and permeability characteristics of the rock.

4.3.2 Controls on Feldspar Distribution

There are several probable explanations for the differences in distribution of the feldspar within and between PH-102 and PH-250. One important influence on feldspar distribution is initial source areas. It is possible that the source areas varied for different parts of the channel sandstone body, which is really a sequence of numerous channel fills. The rock at the base of

PH-250 is rich in potassium feldspar and metamorphic rock fragments. It could be sourced from a metamorphic area, while rock higher in the stratigraphic column and in PH-102 might be richer in recycled sandstone materials. Related to source area is the question of transport distance. The near absence of feldspar in the fine grained sandstones (FGLP, FGHP) could be related to a longer transport distance and therefore greater sorting than was experienced by the basal PH-250 sandstone (CGLP). Small grains of feldspar are less likely to survive extended transport and are more subject to chemical weathering. The relative immaturity of CGLP indicates a shorter transport distance, which would allow more and larger feldspar grains to be deposited. The presence of large, angular grains (quartz, lithics) in CGLP along with the moderate to poor sorting supports a short transport distance.

Water chemistry and water-rock reactions were probably quite important in determining feldspar content. It is difficult to know the past composition of formation waters in these sandstones, but some estimate can be made from petrographic clues as to diagenetic history. The rocks show early pore-filling by calcite, suggesting an alkaline water chemistry. Some time later the calcite was probably dissolved, and potassium feldspar broke down to form kaolinite, supporting a slightly acidic chemistry. It appears that all of the potassium feldspar in FGHP has been replaced by calcite, or dissolved, and the secondary porosity filled by kaolinite. There is evidence of multiple events of calcite and kaolinite precipitation, for example from order of deposition around framework grains, and inclusions. A very early poikilotopic calcite cement appears to have been deposited before much compaction occurred (for example, LAG). A later calcite occurs as subhedral to euhedral grains within corroded feldspars.

Potassium feldspar has been almost completely replaced in all of the samples studied,

except in the basal PH-250 (CGLP) section and the outburst (OBT) samples. There are two

principal ways in which the corrosion of feldspar could be halted. The first possibility is that there

was a low water/rock ratio in the lower portion of the sandstone body. As diagenesis proceeded

and water circulation through the channel sandstone decreased, the pore water in contact with the

feldspar grains could have become saturated with respect to potassium, and the reaction could

have reached equilibrium. The second possibility is that formation water was displaced by

hydrocarbons, slowing or halting the diagenetic reactions. It is unlikely that water was displaced

early in the diagenetic history, because if this was the case there could not have been later

replacement reactions, for example, kaolinite and calcite growth. Presently, the lower channel

sandstone is locally gas-filled (i.e. outburst), which may explain why the feldspar dissolution

reaction halted. The possibility exists that a combination of low water/rock ratios and water

displacement (gas trapping) mechanisms were at work in the channel sandstones. Differences

between PH-102 and PH-250 might be explained by initial differences in feldspar distribution,

formation-water flow regimes, or in the amount and/or timing of hydrocarbon generation and

migration.

4.3.3 Controls on Kaolinite Distribution

Kaolinite occurs in the samples studied as a breakdown product of feldspars (mainly

potassium feldspar ?). There is uncertainty as to the composition of all the original feldspars

because some of them have been completely replaced by kaolinite. Analyses of corroded grains,

however, show that they are potassic (Appendix D). Kaolinite growth is one of the later steps in

diagenesis, along with the formation of illite and sericite as alteration products. As mentioned in

the previous section, however, it is possible that there was more than one episode of kaolinite

growth. Much of the distribution of kaolinite can be explained by the original distribution of

potassium feldspar. In PH-102 kaolinite is common and well distributed. Upon close

examination of some pores small amounts of corroded potassium feldspar can be seen, suggesting

that the pore spaces (and kaolinite pore-filling) represent the previous occurrence of potassium

feldspar. In PH-250 kaolinite is found along cracks, grain boundaries, and cleavages of corroded

feldspars, supporting these grains as the source of kaolinite mineralization. If the original

sediments were rich in feldspar, then one would expect that, following diagenesis, the rocks

would be rich in kaolinite if appropriate groundwater chemistries were present. In short, the

current abundance of kaolinite in FGHP probably represents a relatively high feldspar

concentration before diagenesis. It should also be noted that the amount of kaolinite that grows

in a rock will be limited by the original pore space. If FGHP rocks were initially more porous

than CGLP rocks, then one would expect them to have had more space available for kaolinite

growth.

Additional controls on kaolinite distribution are the conditions that control the chemical

reactions leading to feldspar breakdown, mainly water chemistry. The formation waters of Phalen

Colliery are slightly acidic at present. If this condition was present earlier in the diagenetic

history, breakdown of potassium feldspar to kaolinite may have occurred by the following

reaction:

$$2KAlSi_3O_8 + 2H_2CO_3 + 9H_2O = Al_2Si_2O_5(OH)_4 + 4H_4SiO_4 + 2HCO_3^- + 2K^+$$

(K-feldspar)   (carbonic acid)   (kaolinite)
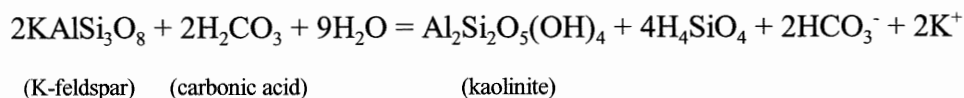
(Schwartz and Longstaffe, 1988)

There are several reactions that explain the breakdown of K-feldspar to kaolinite, but this reaction

seems probable due to the ready source of carbonic acid in a coaly environment. Some of the K-

feldspars were partially replaced by calcite, which suggests that several reactions may have

occurred between the rocks and formation water of the channel sandstone over time. It is difficult

to relate the mineralogy of the channel sandstone to the chemical composition of modern brines at

the mine. The history of brine formation and migration is not yet fully understood, and there is

not enough detailed chemical data from the channel sandstone minerals to form any reliable

hypotheses as to the nature of this water/rock relationship. It is possible that, at least in PH-102,

there was a local influence on formation water chemistry due to the limestone overlying the

channel sandstone.

The differences in kaolinite distribution between PH-102 and PH-250 (especially basal

PH-250, CGLP) are probably due to original differences in porosity, possibly as a result of lithic

compaction. In PH-102, which probably has higher porosity and permeability, the water rock

ratio would have been higher than in CGLP, which has very restricted porosity. The larger

volume of water moving through PH-102 (mainly FGHP) may have allowed the feldspar

dissolution reactions to go to completion, whereas in PH-250 (basal) they were halted before

complete dissolution could occur. This is suggested by the differences in the amount of corroded

feldspar left between PH-102 and PH-250. The feldspar in PH-102 and upper sections of PH-250

is almost completely replaced.

4.3.4 Summary of Controls

There are several controls on the distribution of lithics, feldspar, and kaolinite. Some of

these relate to initial deposition, sorting, and transport, while others have more to do with

diagenetic mechanisms.   Few assumptions can be made about the diagenetic history of

Merlebach or #26 Colliery, because only one sample from each was examined in this study.

AGAT (1995) proposes the following summary of diagenetic history for PH-250, which

presumably is not greatly different from the history of PH-102:

> 1) Precipitation of pyrite, quartz overgrowths, and rimming siderite
>
> 2) Dissolution of feldspar, precipitation of kaolinite, calcite, and dolomite
>
> 3) Subaerial exposure (?) and sericitization of aluminosilicates (not covered by this author)

The diagenetic history of the channel sandstone is quite complex. Figure 4.6 shows a summary of

diagenetic history for the channel sandstone as inferred from the present study. In the first stage,

there was probably also precipitation of the poikilotopic calcite cement. Mechanical compaction

is very important in these rocks, and occurred early in the history, before stage #2. Feldspar

dissolution to kaolinite typically occurs under conditions of low pH, whereas dissolution to calcite

typically occurs under somewhat higher pH conditions (Faure, 1991), suggesting a possible

difference in timing between these two events. There is evidence in the rocks for more than one

generation of calcite/kaolinite growth. Section 5.2.0 discusses further work that could contribute

to a better understanding of the diagenetic history of the Phalen channel sandstone.

4.4.0 General Summary of Effects on Porosity and Permeability

4.4.1 Porosity

The density logs obtained to date can be correlated to the stratigraphic logs (Figure 3.16,

3.17). The resolution, however, is not great enough to make the MST a useful instrument for

determining outburst risk. At best it can be used to distinguish general lithologies, such as

Figure 4.6 Summary of diagenetic history of Phalen channel sandstones. Compaction and cementation were early, followed by a stage of feldspar dissolution, then clay and calcite precipitation. Relative timing of the calcite/dolomite/kaolinite precipitation is uncertain. Gas entrapment was late.

sandstones from siltstone or limestone. This equipment cannot be used to determine permeability of a core (most important in outburst studies) and detailed petrographic work is still necessary. The MST is time-consuming to use, and probably is not suited to this type of study.

Porosity varies somewhat through the individual cores, but for PH-250 it is on average 2% lower than for PH-102 (Figure 3.18). Two distinct patterns of porosity emerged during the course of petrographic description and point counting: 1) evenly distributed, intergranular, with associated kaolinite pore filling, and 2) isolated, intragranular, associated with corroded potassium feldspar grains. Groups CGLP and OBT were the only two to show significant intragranular porosity, whereas FGHP shows predominantly intergranular porosity. The type of porosity is important in that it will strongly influence the permeability of the sample. Outburst rocks consistently show isolated corroded feldspar grains with intragranular porosity, and very low permeability. Rocks apparently less prone to outburst are dominated by intergranular porosity.

4.4.2 Permeability

Permeability values obtained from PH-250 were, on average, an order of magnitude lower than values obtained for PH-102 (Figure 3.20). This is due largely to the nature of the porosity (very isolated intragranular) within PH-250. Samples PH-102-5 (LAG) and PH-102-13 (FGLP) have permeabilities that are two orders of magnitude higher than all other measurements. In thin section there is very little to distinguish these sections from others in the same groups (e.g. amount of epoxy absorbed, pore fillings), and as yet there is no explanation for why these values are so high. Based on visual estimates, permeability for the outburst rocks is very low. Permeability in the channel sandstone is at least partially associated with the amount of kaolinite and especially the amount of corroded feldspar in the rock. Because of the restricted permeability

criteria for outburst occurrence, PH-250 is considered to be at a higher risk of outburst than PH-102. In the event of sudden depressurization due to mining, gas escape from PH-250 would be greatly restricted by the low permeability.   Figure 4.7 shows the relationship between porosity and permeability for the Phalen samples (note that no numerical data for porosity and permeability were available for the outburst rocks, OBT). There appears to be a moderate positive correlation overall, but the individual petrographic groups show good to poor clustering. This graph is, however, misleading. The samples from FGLP and CGLP plot very close together, suggesting that FGLP is as prone to outbursting as CGLP. In fact, the porosity distribution is quite different between these two rocks, although the permeability values are similar (low). CGLP shows isolated porosity, whereas FGLP has low but relatively evenly distributed porosity. FGLP is very poor in kaolinite (approximately 1%), and although AGAT reports an average porosity of 7.2%, there is a distinct lack of blue epoxy in this section. The isolation of porosity (intragranular), along with restricted permeability, probably puts a rock at a higher risk for outbursts. The reliability of Figure 4.7 could be increased by using a larger sample set.

4.5.0 Comparison of Phalen to Other Coal Mine Outbursts

It is important to note that not all outburst rocks will show a distinctive petrographic character and porosity/permeability in the way that PH-250 and the outburst samples do. When outburst sandstones from No. 26 Colliery and non-outburst sandstones from Lingan Colliery were compared no major mineralogical differences were noted, although both had extremely low permeability (Corelab Canada, 1986). Table 4.1 summarizes average porosity values for outburst rocks from Phalen Colliery, #26 Colliery, and Ibbenburen (Germany).
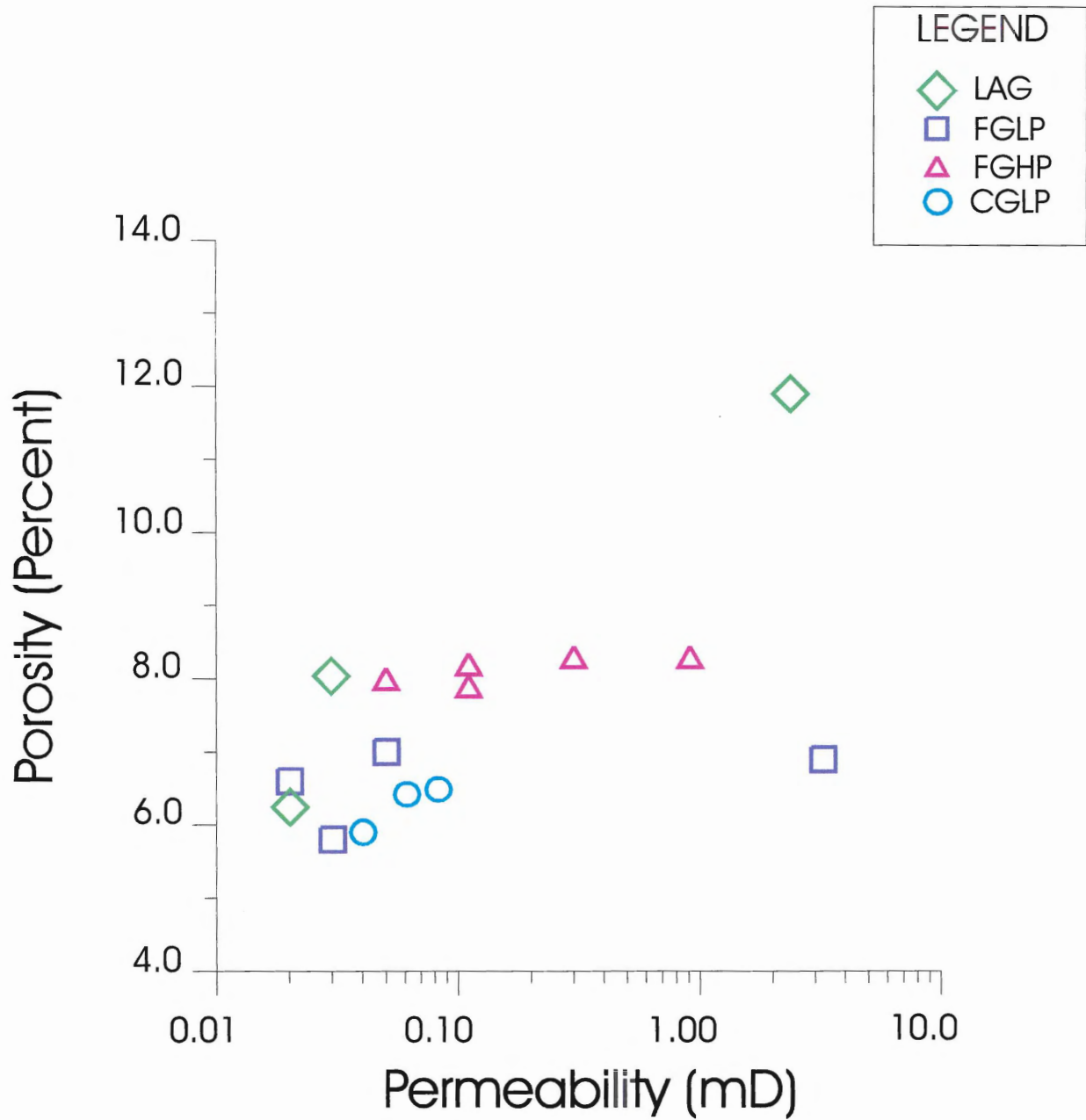
Figure 4.7 Graph of porosity vs. permeability for Phalen samples, by petrographic group.

Table 4.1 Summary of average porosity values for outburst rocks from Phalen, #26, and Ibbenburen collieries.

Colliery	Porosity (average)	Source
Phalen, PH-250	6.5%	AGAT (1995)
Phalen, PH-102	8.5%	AGAT (year unknown)
#26 Colliery	5.24%	Aston et al. (1990)
#26 Colliery	4.7%	Gorski (1984)
Ibbenburen	10% - 14% (<7% did not burst)	Aston et al. (1990)

In the case of the Phalen mine the outburst sandstones are readily distinguishable in hand specimen from rocks interpreted to be at a lower risk for outbursts. Rocks from Lingan and No. 26 are different from the outburst sample from Phalen and basal PH-250 in that they are mature, fine-grained rocks. Little detailed petrographic work has been done in the Phalen, Lingan, or #26 collieries, except for reports by AGAT Laboratories, and work summarized by P. Cain (personal communication, 1996). There does not seem to be a characteristic porosity value for outburst prone (or actual outburst) rocks, although low permeability is important. The combination of low permeability and isolated porosity was important in all of the outburst rocks studied (Phalen, #26, and Merlebach, France).

4.6.0 Visual and Petrographic Indicators of Relative Outburst Potential

There are several indicators that could provide useful indicators of outburst risk at the Phalen Colliery. The rocks that are inferred to be the most outburst-prone (CGLP) and the rocks that have outburst (OBT) are grey in colour, and coarse to very coarse-grained. Large white (kaolinitic) feldspar grains (approximately 1 mm) are usually visible. Petrologic description shows

further characteristics that are distinctive of the Phalen outbursts. Most important of these

characteristics are isolated corroded feldspar grains. The presence of isolated kaolinite patches or

compacted lithic fragments are inferred to be secondary indicators of outburst risk. Alone, they

are not reliable indicators of outburst risk, but are important when found with corroded feldspar.

Most important in determining outburst risk, from a petrographic point of view, is low

permeability. There is a significant variation in porosity of outburst sandstones, and what

explodes in one mine will not necessarily explode in another (e.g. see Table 4.1, compare the

Cape Breton mines with rocks from Ibbenburen). The combination of low permeability and

isolated porosity is key, because it creates a variety of stratigraphic traps for pressurized gas,

which is a main component of outburst risk.

Chapter 5 Conclusions

5.1.0 Petrography, Porosity, Permeability, and Outburst risk

From this work on petrology, porosity, and permeability, I was able to draw several major conclusions about the Phalen channel sandstones:

1) All of the outburst rocks studied and samples proximal to the 1994 outburst (basal PH-250, CGLP) were relatively rich in corroded potassium feldspar, whereas the core distal to the site of the major Phalen outburst (PH-102) had less than 1% corroded feldspar.

2) There are several petrographic characteristics of the Phalen channel sandstone that contribute to decreased permeability and, therefore, to increased outburst risk. These include mechanical compaction of lithic grains, pore-filling cementation (calcite and kaolinite), and isolated intragranular porosity.

3) Corroded potassium feldspars provide isolated intragranular porosity in the channel sandstone, which acts as a low permeability gas reservoir in which gas is trapped. The low permeability confines gas during expansion from mining, causing explosive failure of the rock.

4) Rock in the vicinity of core PH-250 is inferred to be more prone to outburst than rock near PH-102, due to corroded feldspar content, restricted distribution of pore-filling kaolinite, low permeability, isolated porosity and general similarity (e.g. immature, poorly sorted) to actual outburst sandstones.

5)   Diagenesis has an important influence on outburst risk, as it controls permeability

through distribution of corroded feldspar and kaolinite, compaction, and cementation

history. Initial low permeability is interpreted to restrict water/rock interactions, and

prevent total degradation of feldspars. This may be assisted by the cessation of diagenetic

reaction following gas entrapment.

6)   If a mine is known to satisfy several requirements for outburst initiation (e.g. high gas

pressure, high rock stress, brittleness), the detailed petrography can be used to determine

relative outburst risk.

7)   Corroded feldspars may provide a useful warning sign of outburst risk in the Phalen

channel sandstone, and in similar channel sandstones worldwide, that can be readily

assessed in hand specimen.

5.2.0 Future Work

Knowledge of rock/gas outbursts at the Phalen Colliery could be improved through

further examination of the channel sandstone, especially those rocks known to have experienced

outbursts. Studies such as this could be compared with detailed data from other mines, and

possibly used to identify general characteristics of outburst-prone strata. In order to better

understand the diagenetic history, more work must be done on the detailed chemistry of the

Phalen channel sandstones. Several techniques would be appropriate for studying diagenetic

history, including staining, electron microprobe, cathodoluminescence, and isotopes. Data

obtained with these techniques would also allow the channel sandstone mineralogy to be related

to the chemistry of the formation waters.

References

AGAT Laboratories. 1995. A petrographic study of five samples from Phalen Colliery. Work Order No. A-5402. November.

Aston, T., Kullman, D., and Barron, K. 1990. Modelling of outbursts at #26 Colliery, Glace Bay, Nova Scotia; Part 1: Outburst history and field data. Mining Science and Technology, 11:253-260.

Belin, J. 1981. Prevention of instantaneous outbursts of methane and coal or rock. CEC Safety and Health Commission for the Mining and Other Extractive Industries, Working Party on Ventilation, firedamp and other Mine Gases Report OP 324 Doc 6093/81, Study No. 5/80/267/(123), Luxembourg, 1981.

Cape Breton Development Corporation, Phalen Colliery. 1994. Risk Assessment Report, Volume 1.

Cape Breton Development Corporation, Phalen Colliery. 1994. Risk Assessment Report, Volume 2.

Corelab Canada Ltd. 1986. Petrographic study of outburst material, Sydney coalfield, N.S. Final Report by Corelab Canada to CBDC, File No. 70687-86-128.

Cyrul, T. 1993. Prediction of rock and gas outburst occurrence. Engineering Geology, 33: 241-250.

Faure, G. 1991. Principles and Applications of Inorganic Geochemistry. New York: MacMillan Publishing Company, 626 p.

Folk, R.L. 1968. Petrology of sedimentary Rocks. Austin, Texas: Hemphill's Book Store, 170 p.

Gibling, M.R., and Bird, D.J. 1994. Late Carboniferous cyclothems and alluvial paleovalleys in the Sydney Basin, Nova Scotia. Geological Society of America Bulletin, 106: 105-117.

Gibling, M.R., Boehner, R.C., and Rust, B.R. 1987. The Sydney Basin of Atlantic Canada: an Upper Paleozoic strike-slip basin in a collisional setting. *In* Sedimentary basins and basin-forming mechanisms. *Edited by* C. Beaumont and A.J. Tankard. Canadian Society of Petroleum Geologists, Memoir 12.

Gorski, B., 1984, Laboratory testing of rock cores from No.26 Colliery, Sydney Coalfield. ERP/MRL 84-25(TR), Natural Resources Canada CANMET Divisional Report.

Hacquebard, P.A. 1983. Geological development and economic evaluation for the Sydney coal basin, Nova Scotia. *In:* Current research, part A, Geological Survey of Canada, Paper 83-1A, pp.71-81.

Hart, E. 1936. The shotfirer's manual. London: Charles Griffin and Company, Limited. 128 p.

Jackson, L.J. 1984. Outbursts in coal mines. IEA Coal Research, London. Report #ICTIS/TR25, pp.9-16.

King, L.H., and MacLean, B. 1976. Geology of the Scotian Shelf. Geological Survey of Canada, Paper 74-31, 31p.

Kullmann, D., and Barron, K. 1990. Modelling of outbursts at #26 Colliery, Glace Bay, Nova Scotia; Part 2: Proposed outburst mechanism and model. Mining Science and Technology, **11**: 261-268.

Kullmann, D., and Barron, K. 1990. Modelling of outbursts at #26 Colliery, Glace Bay, Nova Scotia; Part 3: Comparison of model results and field data. Mining Science and Technology, **11**: 269-280.

Rust, B.R., and Nanson, G.C. 1989. Bedload transport of mud as pedogenic aggregates in modern and ancient rivers. Sedimentology, **36**: 291-306.

Rust, B.R., Gibling, M.R., Best, M.A. Dilles, S.J. and Masson, A.G. 1987. A sedimentological overview of the coal-bearing Morien Group (Pennsylvanian), Sydney Basin, Nova Scotia, Canada. Canadian Journal of Earth Sciences, **24**: 1869-1885.

Schwartz, F.W., and Longstaffe, F.J. 1988. Ground water and clastic diagenesis. *In* The Geology of North America, Vol O-2, Hydrogeology. *Edited by*: W. Back, J.S. Rosenshein, and P.R. Seaber. The Geological Society of America, pp. 413-434.

Wightman, W.G., Scott, D. B., Medioli, F. S., and Gibling, M. R. 1994. Agglutinated foraminifera and thecamoebians from the Late Carboniferous Sydney coalfield, Nova Scotia: paleoecology, paleoenvironments and paleogeographical implications. Palaeoclimatology Palaeoecology, **106**: 187- 202.

Appendix A

Environmental Scanning Electron Microscope

The scanning electron microscope uses a focused beam of electrons instead of visible light to produce images with a range of magnifications much greater than the standard petrographic microscope. It provides an opportunity to examine the uncut surfaces of samples, allowing the operator to observe the three dimensional nature of the grain surfaces and relations in geological specimens. Resolutions as fine as 3-6 nm, and magnifications as high as 20 - 150,000x can be achieved with an SEM (Flegler et al., 1993). The environmental SEM (ESEM) was developed to permit analysis of wet samples (generally biological), which cannot be examined with a standard SEM due to the vapor they give off under vacuum. This system offers the advantage of being able to analyze non-conducting surfaces, and therefore eliminates the need to coat samples. The ESEM at B.I.O. also has an attached energy dispersive spectrometry (EDS) detector that allows the operator to view analytical spectra, which are extremely useful in mineral identification. For analysis with the ESEM, chip samples are mounted on aluminum stubs and placed inside the sample chamber, which is then closed and placed under a low vacuum. The chamber is flooded with water vapor and the beam from the electron gun is focused on the sample. Images are produced using cathode-ray tubes and can be captured and stored by an attached computer for later display and processing.

Appendix B

Multi-Sensor Core Logger

The Multi-Sensor Core Logger (MST- multi-sensor track) can be used to determine density and magnetic susceptibility measurements for intact core. Density is determined through the use of a gamma ray source, and susceptibility through a magnetic susceptibility sensor that detects any magnetic material in the core. This process has not previously been used with lithified sediment, and was designed for soft sediment core. Magnetic susceptibility data for the Phalen cores is not used within the thesis.

The procedure used for the Phalen core was as follows. Starting at the stratigraphically highest end of the core, which was labeled "0 cm", the core was divided in the boxes into labeled 92 cm (three foot) sections. After labeling, the core was removed from the boxes and inserted into polycarbonate plastic tubes, cut to 92 cm length. One end of the tube was capped and sealed with tape, and then the cores were saturated with distilled water and the other end sealed. Due to a certain amount of absorption by the core the water level in the tubes was "topped-up" prior to MST analysis.

To analyze the cores they were placed in the "core boat" of the MST, which is pulled conveyor belt fashion by a small computer-controlled motor past the gamma sensor. The gamma ray source is Cesium-137 which is held within a lead housing. A sensor diametrically opposed to the source measures attenuation of the gamma ray at 1 cm intervals as it passes through the centre of the core. The acquired data requires some processing before use, which was carried out by K. Moran and Bedford Institute of Oceanography staff. The MST is calibrated using a core tube

filled with distilled water, and three aluminum disks of varying thickness. Drift measurements are recorded frequently, usually once before analyzing the cores, and once when they have all been run.

Appendix C

Point Count Data

Point count data from Phalen (PH250, PH102, OBST), #26 (PHUN), and Merlebach Colliery (M-1), in percent.

sample	pet. group	quartz	lithics	feldspar	corroded feldspar	opaques	muscovite	clay matrix*	kaolinite	siderite**	calcite	alteration to clay	porosity (count)	porosity (AGAT)
PH250-1	CGLP	63.8	12.8	0.0	3.2	1.6	0.2	1.2	3.6	7.4	2.0	3.6	0.6	6.4
PH250-3	CGLP	54.4	19.6	0.2	6.0	1.0	0.2	3.2	6.8	3.2	3.4	1.2	0.8	6.5
PH250-5	CGLP	56.6	11.4	2.2	0.2	1.4	1.4	5.2	7.0	12.0	0.0	2.6	0.0	5.9
PH250-6	FGLP	60.2	9.4	0.2	0.4	4.4	0.4	8.2	0.8	1.8	0.0	13.8	0.4	5.8
PH250-10	LAG	24.6	3.2	0.2	0.2	0.6	0.2	6.6	0.6	28.6	35.2	0.0	0.0	6.3
PH250-12	FGLP	70.0	3.8	0.2	0.0	0.4	0.0	7.2	2.2	3.8	2.4	9.8	0.2	7.0
PH250-15	FGLP	68.4	4.0	0.4	0.0	1.2	0.0	9.2	1.2	3.8	4.4	7.2	0.0	6.6
PH102-1	LAG	39.6	7.4	0.0	0.0	10.6	0.0	3.6	3.4	16.6	15.4	1.6	1.8	8.0
PH102-3	FGHP	63.6	1.6	0.2	0.0	0.4	0.0	6.0	8.8	5.4	0.8	13.0	0.0	8.0
PH102-5	LAG	58.2	9.6	0.4	0.0	1.2	0.0	4.4	1.2	12.0	6.8	5.0	0.6	12.1
PH102-6	FGHP	67.6	5.4	0.2	0.2	0.2	0.0	5.8	6.4	1.2	2.4	9.2	1.2	7.9
PH102-9	FGHP	63.2	7.6	0.0	0.4	1.2	0.0	4.0	12.2	2.4	2.6	6.2	0.2	8.2
PH102-11	FGHP	57.6	6.4	0.4	0.2	1.4	0.0	6.2	14.0	3.4	1.2	7.6	1.6	8.3
PH102-12	FGHP	61.8	6.0	0.2	0.8	0.8	0.0	4.4	11.6	0.6	6.2	7.4	0.2	8.3
PH102-13	FGLP	75.6	3.2	0.4	0.6	1.2	0.0	5.8	0.4	8.8	0.2	3.8	0.0	6.9
PHUN	OBT	64.6	13.2	0.2	2.6	0.2	0.0	4.6	6.8	5.0	0.0	2.0	0.8	N/A
OBST	OBT	62.0	8.2	0.0	3.6	2.4	1.0	5.6	6.2	5.0	2.6	3.4	0.0	N/A
M-1	OBT	72.0	9.6	0.0	5.8	0.0	0.4	3.0	4.2	0.6	1.8	2.6	0.0	N/A

* apparently unaltered
** includes clasts and cements

Appendix D

Summary of Microprobe Data

Quartz

Element	ZAF	%ELMT	ST.DEV	ATOM.%		%OXIDE	FORMULA
SiKA	1.094	3.976	.031	32.994	SiO_2	8.505	.495
AlKA	1.024	.018	.010 <2sd	.157	Al_2O_3	.034	.002
P KA	.734	.024	.013 <2sd	.179	P_2O_5	.054	.003
O KA		4.576		66.670			1.000
Total		8.593		100		8.593	.5

Albite

Element	ZAF	%ELMT	ST.DEV	ATOM.%		%OXIDE	FORMULA
SiKA	.974	31.477	.098	23.267	SiO_2	67.335	.376
AlKA	.974	10.249	.068	7.888	Al_2O_3	19.367	.127
MgKA	1.038	.047	.046 <2sd	.040	MgO	.078	.001
NaKA	.978	7.487	.082	6.762	Na_2O	10.093	.109
K KA	.983	.096	.030	.051	K_2O	.116	.001
P KA	.748	.076	.042 <2sd	.051	P_2O_5	.173	.001
O PA		47.730		61.940			1.00
Total		97.162		100			.614

Corroded potassium feldspar

Element	ZAF	%ELMT	ST.DEV	ATOM.%		%OXIDE	FORMULA
SiKA	1.012	29.903	.094	23.059	SiO_2	63.969	.374
AlKA	1.014	9.636	.065	7.736	Al_2O_3	18.208	.126
FeKA	.974	.133	.070 <2sd	.051	FeO	.171	.001
NaKA	.933	.498	.049	.469	Na_2O	.672	.008
K KA	1.003	12.756	.083	7.067	K_2O	15.366	.115
BaLA	.816	.235	.149 <2sd	.037	BaO	.263	.001
O		45.486		61.580			1.000
Total		98.648		100			.624

Corroded potassium feldspar

Element	ZAF	%ELMT	ST.DEV	ATOM.%		%OXIDE	FORMULA
SiKA	1.011	28.746	.093	23.040	SiO_2	61.492	.373
AlKA	1.015	9.409	.064	7.852	Al_2O_3	17.778	.127
FeKA	.974	.144	.070 <3sd	.058	FeO	.186	.001
MnKA	.880	.122	.063 <2sd	.046	MnO	.145	.001
MgKA	1.093	.044	.038 <2sd	.041	MgO	.073	.001
NaKA	.933	.436	.049	.427	Na_2O	.588	.007
K Ka	1.002	11.622	.080	6.692	K_2O	14.000	.108
NiKA	.823	.121	.101 <2sd	.046	NiO	.154	.001
ClKA	.997	.033	.027 <2sd	.021	Cl	.033	.000
P KA	.780	.066	.042 <2sd	.048	P_2O_5	.151	.001
O KA		43.867		61.728			1.000
Total		94.600		100		94.600	.620

Corroded potassium feldspar

Element	ZAF	%ELMT	ST.DEV	ATOM.%		%OXIDE	FORMULA
SiKA	1.014	29.565	.094	22.929	SiO_2	63.246	.373
AlKA	1.017	9.604	.065	7.755	Al_2O_3	18.148	.126
MgKA	1.096	.048	.038 <2sd	.043	MgO	.079	.001
NaKA	.934	.375	.049	.355	Na_2O	.505	.006
K KA	1.003	13.386	.085	7.458	K_2O	16.125	.121
Cl KA	1.000	.030	.027 <2sd	.018	Cl	.030	.000
O KA		45.125		61.441			1.000
Total		98.133		100		98.133	.628

Corroded potassium feldspar

Element	ZAF	%ELMT	ST.DEV	ATOM.%		%OXIDE	FORMULA
SiKA	1.015	29.764	.094	23.637	SiO_2	63.670	.382
AlKA	1.010	8.653	.063	7.154	Al_2O_3	16.350	.116
FeKA	.974	.290	.073	.116	FeO	.373	.002
MgKA	1.088	.140	.040	.129	MgO	.233	.002
CaKA	.947	.168	.042	.094	CaO	.236	.002
NaKA	.930	.492	.052	.478	Na_2O	.664	.008
K Ka	1.002	11.323	.079	6.460	K_2O	13.640	.104
ClKA	.996	.030	.027 <2sd	.019	Cl	.030	.000
BaLA	.817	.305	.145 <3sd	.050	BaO	.341	.001
O KA		44.370		61.863			1.000
Total		95.536				95.536	.616

Corroded potassium feldspar

Element	ZAF	%ELMT	ST.DEV	ATOM.%		%OXIDE	FORMULA
SiKA	1.012	29.617	.094	22.959	SiO_2	63.356	.373
AlKA	1.014	9.588	.065	7.739	Al_2O_3	18.117	.126
NaKA	.931	.434	.050	.411	Na_2O	.584	.007
K KA	1.004	13.192	.084	7.347	K_2O	15.892	.120
BaLA	.816	.264	.148 <2sd	.042	BaO	.293	.001
LaLA	.653	.144	.134 <2sd	.023	La_2O_3	.169	.000
O KA		45.174		61.480			1.000
Total		98.411		100			.627

Corroded potassium feldspar

Element	ZAF	%ELMT	ST.DEV	ATOM.%		%OXIDE	FORMULA
SiKA	1.012	29.954	.094	22.947	SiO_2	64.077	.373
AlKA	1.014	9.751	.065	7.778	Al_2O_3	18.426	.126
CaKA	.945	.062	.041 <2sd	.033	Ca	.087	.001
NaKA	.933	.480	.050	.449	Na_2O	.647	.007
K Ka	1.003	12.984	.084	7.145	K_2O	15.640	.116
BaLA	.816	.356	.149 <3sd	.056	BaO	.398	.001
P KA	.782	.060	.042 <2sd	.042	P_2O_5	.138	.001
O KA		45.765		61.550			1.000
Total		99.412		100		99.412	.625

Corroded potassium feldspar

Element	ZAF	%ELMT	ST.DEV	ATOM.%		%OXIDE	FORMULA
SiKA	1.013	29.697	.094	23.036	SiO_2	63.528	.374
AlKA	1.015	9.594	.065	7.748	Al_2O_3	18.128	.126
NaKA	.932	.344	.049	.326	Na_2O	.464	.005
K Ka	1.003	12.779	.083	7.122	K_2O	15.394	.116
CrKA	.818	.073	.055 <2sd	.030	Cr_2O_3	.106	.000
BaLA	.816	.214	.145 <2sd	.034	BaO	.238	.001
LaLA	.653	.135	.131 <2sd	.021	La_2O_3	.158	.000
P KA	.782	.062	.042 <2sd	.043	P_2O_5	.142	.001
O KA		45.261		61.639			1.000
Total		98.158		100		99.412	.622

Corroded potassium feldspar (Center of Grain)

Element	ZAF	%ELMT	ST.DEV	ATOM.%		%OXIDE	FORMULA
SiKA	1.013	29.640	.094	22.915	SiO_2	63.406	.373
AlKA	1.017	9.730	.065	7.831	Al_2O_3	18.385	.127
MnKA	.879	.067	.064 <2sd	.027	MnO	.087	.000
NaKA	.935	.414	.049	.391	Na_2O	.558	.006
K KA	1.003	13.248	.084	7.358	K_2O	15.958	.120
O		45.295		61.478			1.000
Total		98.394		100			.627

Corroded potassium feldspar (Edge of Previous Grain, albite rim?)

Element	ZAF	%ELMT	ST.DEV	ATOM.%		%OXIDE	FORMULA
SiKA	.975	31.952	.099	23.360	SiO_2	68.352	.377
AlKA	.975	10.253	.068	7.805	Al_2O_3	19.374	.126
FeKA	.970	.067	.066 <2sd	.025	FeO	.087	.000
NaKA	.978	7.518	.082	6.716	Na_2O	10.135	.108
K KA	.983	.233	.031	.122	K_2O	.280	.002
P KA	.748	.043	.042 <2sd	.028	P_2O_5	.098	.000
O		48.259		61.943			1.000
Total		98.326		100		98.326	.614

Corroded potassium feldspar

Element	ZAF	%ELMT	ST.DEV	ATOM.%		%OXIDE	FORMULA
SiKA	1.012	29.697	.094	22.848	SiO_2	63.528	.372
AlKA	1.014	9.693	.065	7.764	Al_2O_3	18.315	.126
FeKA	.974	.113	.070 <2sd	.044	FeO	.145	.001
MgKA	1.092	.074	.039 <2sd	.066	MgO	.123	.001
NaKA	.933	.491	.050	.461	Na_2O	.661	.008
K KA	1.004	13.356	.084	7.382	K_2O	16.088	.120
LaLA	.653	.157	.132 <2sd	.024	La_2O_3	.184	.000
O		45.465		61.410			1.000
Total		99.045		100		99.045	.628